Targeting B-RAF Mutated Sarcomas

Sarina Gouravan

Master thesis at School of Pharmacy
Department of Pharmaceutical Bioscience
Faculty of Mathematics and Natural Science
45 credits

Department of Tumor Biology
Institute for Cancer Research
The Norwegian Radium Hospital
Oslo University Hospital

UNIVERSITY OF OSLO

May 2017

Targeting B-RAF Mutated Sarcomas

Sarina Gouravan

Thesis for the Master degree of Pharmacy
Department of Pharmaceutical Bioscience
Faculty of Mathematics and Natural Science
University of Oslo

Supervisors:

Professor Rigmor Solberg & Harald Thidemann Johansen

The thesis is carried out at

Department of Tumor Biology, Institute for cancer research
Norwegian Radium Hospital
Oslo University Hospital

Supervisors:

Professor Ola Myklebost,
Post.docs Else Munthe and Eva Wessel Stratford

Oslo University Hospital
Norwegian Radium Hospital

May 2017

2017

Targeting B-RAF Mutated Sarcomas

Sarina Gouravan

http://www.duo.uio.no/

Trykk: Reprosentralen, Universitetet i Oslo

Abstract

Introduction: Sarcomas are rare cancers, consisting of a variety of subtypes. In general, standard of care is surgery sometimes combined with traditional chemotherapy and/or radiotherapy. Clinical outcome is poor, and there is a critical need for new therapeutics. Recently, the B-RAF^{V600E} mutation was found in several sarcomas by next generation sequencing. Several inhibitors targeting the B-RAF^{V600E} mutation are approved for clinical treatment of metastatic melanoma, opening for drug repurposing and a personalized medicine approach. In this study, we investigated the preclinical efficacy of targeting B-RAF^{V600E} mutations in sarcoma cell lines with the two drugs vemurafenib (B-RAF^{V600E}-selective inhibitor) or RO5126766 (inhibitor of all RAF isoforms and MEK1 kinase). **Methods**: Two liposarcoma cell lines (SA-4 and SW872), one synovial sarcoma cell lines (SW982) and one Ewing's sarcoma cell line (A673) were found to express the B-RAF^{V600E}mutation. Response to targeted therapy was evaluated by monitoring effects on cell growth. The effect on the responding cell line SA-4 was further elucidated by apoptosis assay, cell cycle analysis and drug removal assays. Two B-RAF^{V600E} mutated melanoma cell lines (A375 and WM9) and one liposarcoma (LPS510) without the mutation were included as control cell lines. **Results**: Vemurafenib and RO5126766 induced significant growth inhibition of the SA-4 cell line. Furthermore, although vemurafenib induced apoptosis in a subset of SA-4 cells, a G1-cell arrest appeared to be the main mechanism for growth inhibition in these cells during short-term treatment. In addition, the SA-4 cells were able to regrow following removal of vemurafenib indicating a reversible inhibitory effect. For the remaining sarcoma cell lines, a minor growth inhibition was observed following treatment with either inhibitor, indicating a resistance to therapies targeting B-RAF^{V600E} proteins. **Conclusion**: SA-4 was the sarcoma cell line with the greatest response to B-RAF inhibition. However, the growth inhibitory effect was reversible following removal of vemurafenib. The other three B-RAF mutated sarcoma cell lines analyzed in the study displayed only a minor response to either inhibitor. The lack of response indicates that these three cell lines are not dependent solely on the MAPK pathway for cell growth. The search for effective targeted therapy should therefore extend to other essential pathways or cellular mechanisms essential for sarcoma progression.

Acknowledgements

The thesis presented here was carried out at the Department of Tumor Biology, Institute for Cancer Research at the Norwegian Radium Hospital, Oslo University Hospital in the time period June 2016 to May 2017. I have many people to thank who supported me during my work.

First, I must express my sincere gratitude to Professor Ola Myklebost, who welcomed me the very first day when I walked into the Department of Tumor Biology with nothing but an ambition to do my master thesis in the field of cancer. Your enthusiasm when you presented a potential project to me made me look forward to get started on my thesis.

To Else and Eva, I am truly grateful for you guidance during my thesis work. Your passion and knowledge in the field of cancer research have inspired me, both personally and academically. Your encouragement has given me the motivation to keep working on my project and reach for my goals. Else, you have always been there to help me, no matter what. Both your theoretical knowledge in the field and practical knowledge in the laboratory have been crucial to my success. Eva, you have always helped me stay on track and keep deadlines. I truly appreciate your help in the process of writing my thesis, especially when it comes to English grammar and terminology.

I would like to thank Rigmor and Harald for being my internal supervisors from the Institute of Pharmacy and for answering my questions throughout the process. I would also thank my fellow students and group members for your continuous support and inspirational discussions.

To my grandmother; the fact that you believed in me, helped me reach my goals even though you passed away right before I started my thesis work. To my grandfather; I am grateful for you moral support and for providing me with the resources to keep me going. I also want to thank my parents and sisters, who were cheering for me and helped me unwind during stressful situations.

Finally, I would also like to show my gratefulness to the love of my life that supported me even though he was across the world. Your endless support for my thesis and encouraging words throughout this period has been truly invaluable, especially during the final stage of my work.

Oslo, May 2017 - *Sarina Gouravan*

Table of contents

1 Introduction

1.1 Cancer in general

Cancer is defined as abnormal growth of cells. When a healthy cell loses normal growth control mechanisms due to genetic alterations, this can cause imbalances in signaling pathways which can further lead to cancer. Cancer cells typically have unlimited proliferation and/or resist apoptosis (also called programmed cell death).

When cells grow uncontrollably, a solid mass will eventually form, called a tumor. Tumors can be divided into benign tumors, which are not able to invade adjacent tissues, and malignant tumors, which are invasive. If the malignant cells in addition are able to travel to distant sites of the body and regrow a tumor in the new microenvironment, the tumor is metastatic. More than 100 cancer types have been characterized, and the most common diagnosed cancers worldwide are lung –, breast and colorectal cancers [1]. However, rare cancers, representing one of the largest subgroups as a whole, have worse survival compared to common cancers, and many years of lost lives. Sarcoma is an example of a rare cancer [2, 3].

1.2 Cancer genetics

Cancer is generally defined as disease of the genome, and is presumed to occur through accumulation of several mutations [4-6]. A mutation is defined as any alteration in the genetic material [7]. Mutations can either be inherited through the germ line or acquired as somatic mutations due to DNA damage. Numerous types of mutations have been discovered to play centrals roles in cancers [4, 5]. The genetic alterations range from small aberrations such as point mutations, insertions and deletions, to large-scale alterations such as amplification or deletion of parts of chromosomes or even loss or duplication of entire chromosomes (reviewed in [8]).

Point mutations involve the change in one single nucleotide and can be further categorized based on the effect they exert. “Nonsense mutations” convert an amino acid codon to a stop codon,

which shortens the protein and can further lead to functional loss. “Missense mutations”, on the other hand, changes a single nucleotide so that the codon triplet encodes a different amino acid. In some cases, the mutation does not change the amino acid and is referred to as a “synonymous aberration”. Other types of mutations include *insertions* and *deletions*, which may cause disruption in the open reading frame and the translation of the genetic material. This can further activate or abolish the normal function of the protein [5, 9]. *Chromosomal translocation*, in which an interchange of DNA segments between non-homologous chromosomes occurs, is also a common type of genetic aberration implicated in cancer [4, 10]. Alterations in two types of genes are often involved in cancer development; proto-oncogenes and tumor suppressor genes [6, 7].

An activating mutation in a proto-oncogene leads to a “gain of function” generating an oncogenic protein which can drive the cell towards malignancy. Such a mutation, which can drive tumor progression, is often referred to as a driver mutation, and the associated gene is often referred to as a driver gene. Activation of oncogenes can occur, for instance through single base mutation, gene amplification or chromosomal translocation [6, 7]. The *B-RAF* gene, which is studied in this thesis, is an example of a proto-oncogene that exhibits tumorigenic properties when mutated ($B\text{-}RAF^{V600E}$) [7, 11].

Tumor suppressor genes function as inhibitors of cell growth and are normally activated as a response to oncogenic activity. Inactivation or loss of tumor suppressive function can occur, for instance due to genetic alterations such as missense mutation, insertions or deletions. The “loss of function” might further allow the cell to proliferate in an abnormal fashion, potentially forming a tumor [6, 7, 12]. *TP53* is an example of a tumor suppressor gene frequently mutated in cancer [13].

As mentioned, a cell must gain multiple genetic alterations before it can become cancerous. Cancer is rarely caused by only one mutation, and tumor progression is a gradual process. Often, the cell has one driver mutations, but is latent until the cell loses a tumor suppressor gene or as a consequence of other genomic aberrations. Due to heterogeneity, each tumor will behave uniquely based on the mutations that are present in the tumor.

1.3 Hallmarks of cancer

For a normal cell to become cancerous, the cell must also accumulate a range of specific properties essential for tumorigenesis, known as hallmarks of cancer. Hanahan and Weinberg have proposed ten universal hallmarks of cells which promote tumor growth (**Figure 1.1**). Two of these hallmarks are of high relevance for this study and are described in detail below.

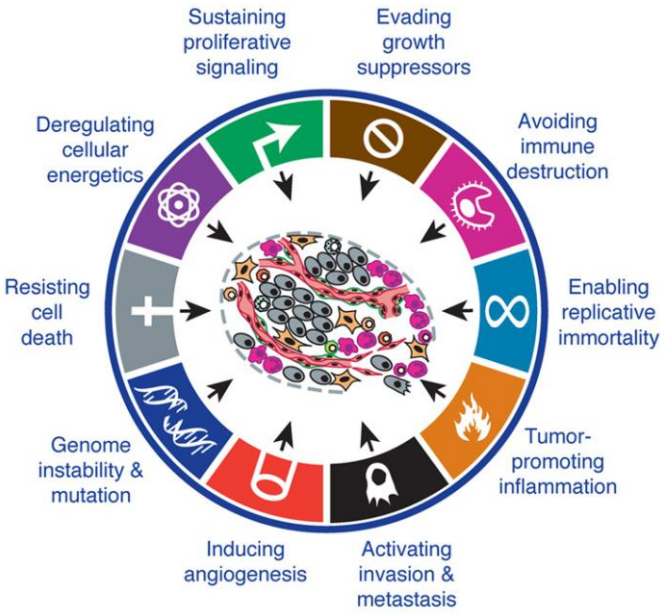

Figure 1.1. Hallmarks of cancer. Characteristics of cells important for cancer. The figure is acquired from Elsevier, Cell [14], copyright 2011.

One hallmark describes the ability of cancer cells to sustain continuous proliferation. In healthy cells, proliferative signals are regulated by growth factors binding to a receptor tyrosine kinase (RTK) which, by activating signaling pathways, stimulate cell growth. Cancerous cells are able to promote sustained proliferative signaling by several mechanisms; for instance by producing growth factor ligands resulting in autocrine proliferative stimulation; or by elevating the number of cell-surface receptors, rendering cells more sensitive to the small amounts of extracellular growth factor ligands. Alternatively, proliferation can be activated by oncogenes as a consequence of somatic mutations in proto-oncogenes. This can result in growth factor independence, rendering cells in a continuous proliferative state [14]. One example is activating mutations in *B-RAF*, resulting in the constitutive activation of the mitogen-activated protein

(MAP)–kinase pathway [14-16]. Furthermore, deregulation of negative feedback loops, such as mutations in RAS onco-protein, can also enhance proliferative signaling [14].

A key hallmark concerns the ability of cancerous cells to resist cell death. Normally, healthy cells would induce senescence or undergo apoptosis as a defense mechanism against excessive growth–promoting signals. Apoptosis is regulated through a complex intracellular machinery involving effector molecules (pro–and anti–apoptotic regulators), which determine whether cells will undergo self-destruction [14]. If so, these effector molecules activate a cascade of proteases called "caspases" [17] that are part of the apoptotic process. However, cancer cells are able to adapt to the excessive signaling and circumvent the induction of apoptosis. One example of resistance to apoptosis is the loss of tumor suppressors, which would normally induce apoptosis in response to unrepairable DNA damage [14] .

Other hallmarks include evasion of growth suppressors, genetic instability which can cause mutations further affecting cell malignancy, and deregulated cellular metabolism. The potential to invade tissue and generate metastasis, induce angiogenesis (vascularization of the tumor), induce tumor-promoting inflammation, enable replicative immortality and the ability to avoid immune destruction are other factors which can contribute to tumor development [14].

Cancer is divided into several subgroups based on their origin. Malignancies of the blood and blood-forming tissues are called leukemias and lymphomas, respectively. Cancerous cells can also form solid tumors, and these are either of epithelial origin (carcinoma) or mesenchymal origin (sarcoma)[1]. Sarcomas are the main focus of this study.

1.4 Sarcoma

Sarcomas are rare tumors with variable characteristics regarding growth rate, incidence, grade of malignancy and prognosis, accounting for about 1 % of all human cancers [3, 18]. More than 50 sarcoma subtypes have been identified by the World Health Organization [19]. The transformed cells are presumed to arise from the mesenchymal linage and are broadly divided into two subgroups; soft tissue sarcoma (STS) comprising fat, muscle, synovium, gastrointestinal tract

[1] https://www.cancer.gov/about-cancer/understanding/what-is-cancer#types-of-cancer

and connective tissue, and cancers arising from bone tissue [3, 20] (**Figure 1.2**). Sarcomas are named after the tissue they resemble [19], where cancers of the bone are called osteosarcoma and cancers or the fat tissue are called liposarcoma (which is one of the most common subtypes of sarcomas)[21, 22]. However, one can also have osteosarcomas arising in soft tissue, and soft tissue tumors may transdifferentiate to osteosarcoma [23]. The annual incidence of bone tissue and soft tissue sarcomas in Norway is 40 and 300, respectively[2]. Diagnosis of soft tissue sarcomas mostly relies on core needle biopsies and histological examination [21].

The incidence of sarcoma subtype varies with age [21], and accounts for up to 10 % of pediatric neoplasms [24, 25]. Some sarcomas occur with higher frequency in children and adolescents, including cancers derived from the skeletal muscle (rhabdomyosarcoma) and bone tissue (osteosarcoma) [20, 25]. In some cases, symptoms are lacking at an early stage, and as a result the disease can be challenging for the physician to identify and characterize. When the patient is finally diagnosed, the disease may be at an advanced stage [21]. Furthermore, few therapeutic options as well as the high incidence in young adults and children results in most years of lost lives compared to common cancers [3]. Traditionally, the main treatment for sarcomas has been surgery combined with radiotherapy (local effects) and/or chemotherapy (systemic effects) for the most aggressive tumors [21, 26]. Pharmaceutical companies have not prioritized to develop treatments for sarcomas. This is partly because the pharmaceutical industry focuses on developing treatment for more common cancers which are economically more beneficial. In addition, the rarity and heterogeneity of sarcomas along with lack of knowledge and expertise make these cancer subtypes challenging to investigate [2, 21].

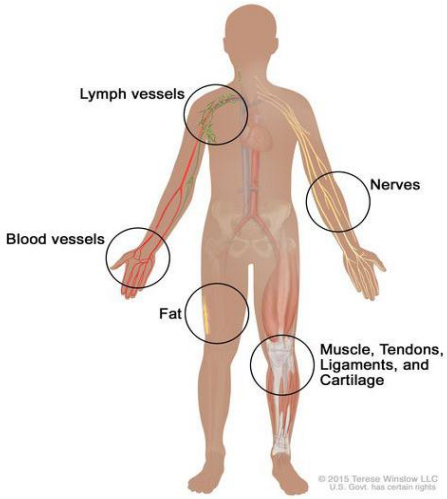

Figure 1.2. Soft tissue sarcoma.
Picture acquired from National Cancer Institute.
URL:https://www.cancer.gov/PublishedContent/Images/images/cancer-types/sarcoma/soft-tissue-sarcoma-article.jpg

[2] www.helsedirektoratet.no Nasjonale faglige retningslinjer – Nasjonalt handlingsprogram med retningslinjerfor for diagnostikk, behandling og oppfølging av sarkom, 03/2015.

1.5 Personalized medicine

To date, the therapeutic strategies have mainly aimed to treat the tumor type rather than the genetic aberration. Personalized medicine, also known as precision medicine or targeted therapy, is based on identifying genetic alterations in the individual tumor, in order to select the optimal treatment for each patient. These genetic alterations are often targetable with already approved drugs for a specific cancer subtype. When the same genetic alteration is found in other cancers, the use of the specific therapeutics is known as repurposing of drugs (**Figure 1.3**). Throughout the last years, next generation sequencing (NGS) has opened new possibilities for comprehensive, genome-wide analysis [27]. It is now more cost-effective and less time-consuming to investigate tumor-specific alterations in the DNA from small amounts of genetic material [27, 28]. NGS has revealed several genetic drivers of cancer [29]. This can enable oncologists to treat patients in a personalized manner with targeted therapeutics [28]. One example of a personalized approach is the use of the tyrosine kinase inhibitor imatinib, originally approved for the treatment of chronic myeloid leukemia (CML). Imatinib targets the Bcr-Abl oncoprotein central to the pathogenesis of CML [30]. Imatinib also showed activity against c-KIT, another driver gene frequently mutated in the sarcoma subtype gastrointestinal stromal tumor (GIST). Imatinib was repurposed for treatment of GIST patients with the c-KIT mutation, which responded well to the treatment with a response rate of 80% versus 10 % following chemotherapy [31]. As a result, Imatinib has been approved as a standard therapy for GIST patients with c-KIT mutations, improving patient survival [32]. This is an example of targeted therapy which has encouraged scientists to further focus on the benefit of personalized medicine and repurposing of drugs.

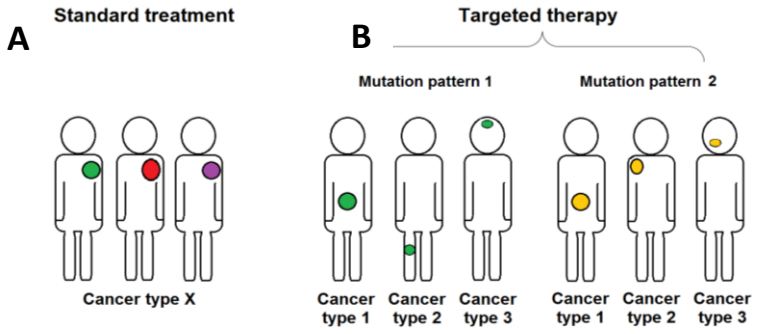

Figure 1.3. Personalized medicine. **A)** Traditional, standard therapy is surgery and chemotherapy/radiotherapy for a specific cancer (X), independent of mutation.

B) Targeted therapy independent of cancer subtype and site, but dependent on mutation, indicated as green and yellow tumors.

1.6 B-RAF and MAPK signaling pathway

The RAF family kinases are serine/threonine kinases and consist of three members (A-RAF, B-RAF and C-RAF). The RAF kinases signal through the mitogen-activate protein kinase (MAPK) signaling pathway which includes the downstream kinases MEK and ERK. The MAPK pathway is a central signaling pathway for transmission of extracellular signals to the nucleus, further regulating cellular processes such as cell growth and survival [33-35].

RAF kinases are normally activated through growth factor signaling, for example from the epidermal growth factor receptor (EGFR). The growth factor binds to its receptor tyrosine kinase on the surface of the cell membrane, which induces dimerization of the receptor and auto-phosphorylation of a tyrosine residue [36] (**Figure 1.4A**). This will in turn recruit adaptor proteins, growth factor receptor-bound protein 2 (GRB2) and the guanine nucleotide exchange factor (GEF). In the MAPK pathway, the GEF is known as sons of sevenless (SOS). SOS further binds and activates membrane-bound RAS (a GTPase) by catalyzing the RAS-GDP to an active GTP-state, introducing a conformational change in RAS. Activated RAS-GTP recruits RAF kinase from the cytosol to the cell membrane [34, 37]. Upon binding of RAF to RAS-GTP, RAF undergoes a conformational change where the kinase domain is relieved from its own auto–inhibitory domain [38, 39]. RAF kinases dimerize either through homo-dimerization or hetero-dimerization, which further induces auto-phosphorylation and subsequently activation of RAF. Activated RAF phosphorylates MEK 1/2 kinases, which further phosphorylate and activate ERK 1/2 kinases. Activated ERK 1/2 kinases phosphorylate a number of cytoplasmic substrates and nuclear transcription factors regulating transcription [34, 37, 39].

B-RAF is the RAF family member with the highest basal activity and affinity to RAS [40]. Recently, B-RAF was found to be frequently mutated in several cancers [11, 16, 41]. The most common B-RAF mutation, accounting for up to 90 % of all B-RAF mutations, involves the substitution of adenine (A) to thymidine (T) at nucleotide 1799. This alteration leads to the substitution of the amino acid valine (V) with glutamic acid (E) at codon 600 (referred to as $B\text{-}RAF^{V600E}$) [16, 37, 42, 43]. The V600 is in the activation segment of the B-RAF protein and important for the auto-inhibition of B-RAF [44]. $B\text{-}RAF^{V600E}$ mutations encode B-RAF proteins without the auto-inhibition. This allows B-RAF to constitutively activate the MAPK pathway as

a monomer, independent of growth factor binding and RAS-GTP stimulation, further driving the proliferation of cancer cells (**Figure 1.4B**)[37, 45-47].

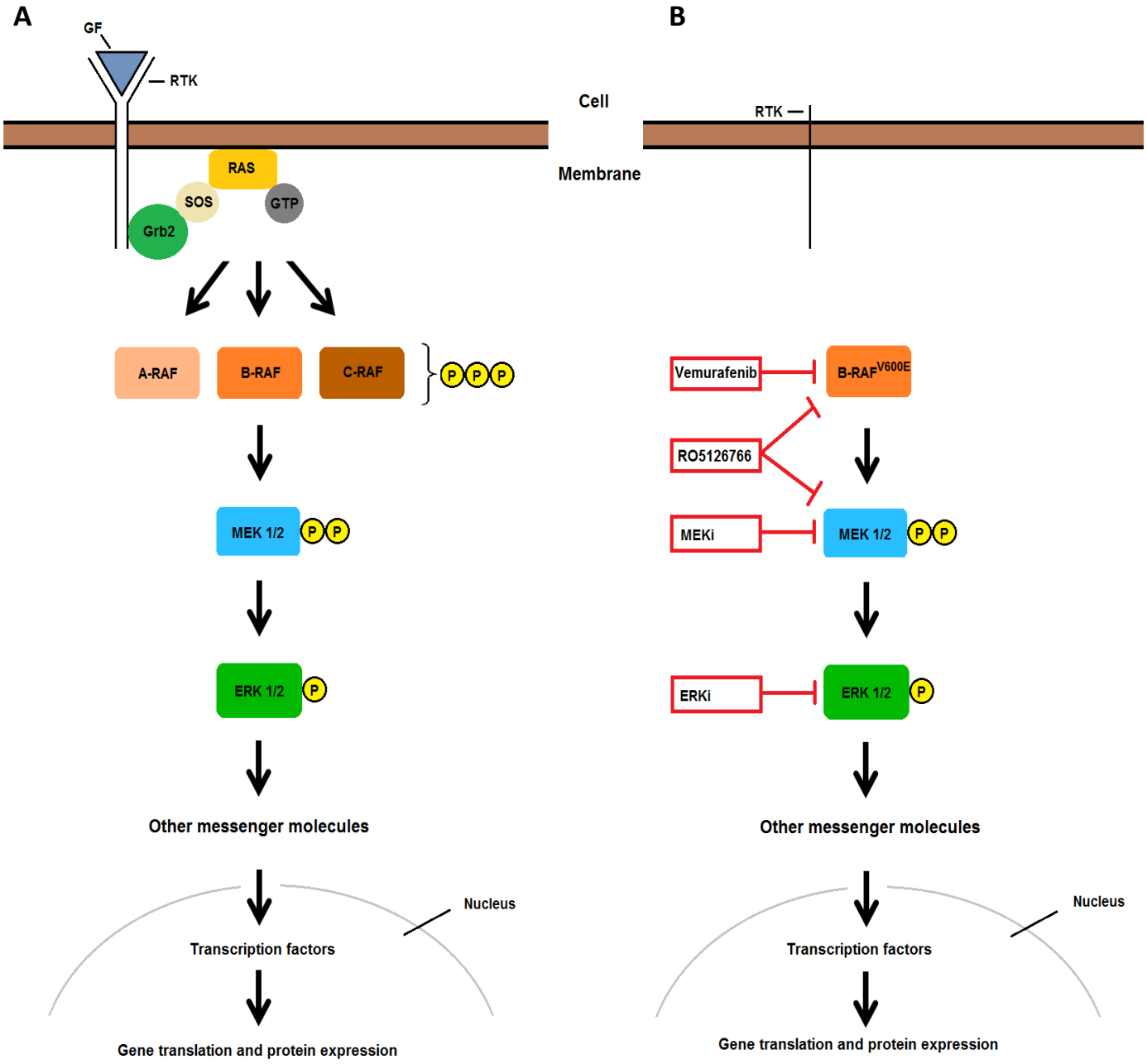

Figure 1.4. MAPK/ERK signaling pathway in normal (A) and cancerous (B) cells. A) In normal healthy cells, signaling is initiated when growth factor (GF) binds to its respective receptor tyrosine kinase (RTK), subsequently inducing a phosphorylation cascade resulting in cellular activity. **B)** Activating mutations in B-RAF (B-RAF^{V600E}) lead to constitutive signaling independent of upstream RTK stimulation by GF. Several components of the MAPK pathway can be inhibited. Inhibitors are indicated in red boxes. Vemurafenib specifically inhibits B-RAF^{V600E} mutated protein. RO5126766 inhibits RAF and its downstream kinase MEK1. Figure adapted from [45].

1.6.1 B-RAF inhibition as a therapeutic strategy

The B-RAF^{V600E} mutation is found in approximately 50 % of all melanoma patients [35]. Accordingly, B-RAF was an attractive target for therapy [45, 48]. Initially, the small molecule inhibitor BAY 43-9006 (sorafenib) was developed, but had higher affinity to C-RAF than B-RAF, resulting in no significant antitumor activity in B-RAF-mutated melanomas [45, 49, 50]. As a result, two protein kinase inhibitors, PLX4032 (also referred to as vemurafenib) and PLX4720 (a vemurafenib analogue) were developed, showing specificity to B-RAF^{V600E} over wild-type B-RAF (B-RAF^{WT}) [45]. Vemurafenib was chosen over PLX4720 for further studies due to higher selectivity and more favorable pharmacokinetic properties [45, 51].

Vemurafenib in treatment of melanomas

Vemurafenib is a first-in-class small molecule inhibitor of the MAPK pathway, which specifically targets B-RAF with the V600E mutation [45, 52, 53]. Vemurafenib binds in an ATP-competitive manner [45, 54] to one of the RAF isoforms in the dimer [55], and has higher affinity to the "active" rather than the "inactive state" of B-RAF [56].

Preclinical testing indicated vemurafenib as a potent, anti-proliferative inhibitor for the treatment of melanoma patients harboring the B-RAF^{V600E} mutation [53]. Encouraged by the effectiveness of vemurafenib in *in vitro* and *in vivo* models, the mutant-specific B-RAF inhibitor proceeded to clinical trials for melanoma patients regardless of the B-RAF-mutation status. Treatment with vemurafenib showed high antitumor activity compared to historically used therapies (the alkylating drug dacarbazine as chemotherapy) [57]. In multiple trials, the response rate was approximately 50 % for patients treated with vemurafenib versus 10-20 % in patients treated with dacarbazine. Furthermore, in a clinical trial the progression-free survival was approximately 7 months for the vemurafenib-treated group versus 2 months for the dacarbazine-treated group. Media overall survival was 84 % for vemurafenib-treated patients versus 64 % for dacarbazine-treated patients [45, 58-61]. Among the most common side effects were arthralgia, rash, fatigue, nausea, alopecia and squamous cell carcinoma (SCC) [62, 63]. In some melanoma patients, however, vemurafenib treatment led to a paradoxical tumor progression. Several reasons have been proposed, including up-regulation of wild-type RAF proteins and activation of MAPK pathway following inhibition of mutated B-RAF [55, 64, 65]. Adverse effects affecting the skin, especially SCC, are thought to be a consequence of this paradoxical activation [66, 67].

Following these incidences, patient tumors were sequenced for the presence of mutations, showing that the responders of vemurafenib treatment had the B-RAF^{V600E}-mutation in the tumor [58, 59]. In melanoma patients with B-RAF^{WT}, inhibition with vemurafenib led to an up-regulation of C-RAF which could drive the signaling towards cell proliferation [65]. In 2011, vemurafenib (Zelboraf) was approved for the treatment of patients with B-RAF^{V600E}-positive unresectable or metastatic melanoma [52, 68]. The standard dosage of 960 mg tablets twice a day was found to be the highest tolerated dose [59, 68].

Vemurafenib in non-melanoma cancers with the B-RAFV600E mutation

The significant improvement in progression-free survival in melanoma patients treated with vemurafenib raised hope for using the selective B-RAF^{V600E} inhibitor as a therapeutic for treatment of non-melanoma cancers harboring the same mutation [69]. Recently, the B-RAF^{V600E} mutation was also found in other cancers, including approximately 10 % of colorectal cancers (CRC) [70, 71] and 80 % of papillary thyroid cancers [72]. In colorectal cancer, B-RAF-mutation is a negative prognostic factor and associated with adverse disease progression and poor clinical outcome [69, 73]. The efficacy of vemurafenib was investigated in patients with metastatic colorectal cancer (mCRC) tumors with the B-RAF^{V600E}-mutation, who did not respond to previous treatments with radiotherapy and/or chemotherapy. Surprisingly, no significant antitumor activity was observed following treatment with vemurafenib in mCRC patients [74]. Moreover, adverse effects such as fatigue, hyperglycemia and toxicities affecting the skin were frequently reported [75, 76]. These disappointing results led to studies in cell lines aiming to understand the lack of efficacy for vemurafenib in colorectal cancer [73]. *In vivo* and *in vitro* tests revealed an up-regulation of epidermal growth factor receptors (EGFRs) upon inhibition of mutated B-RAF in CRC, further driving the signaling towards proliferation. This could explain the lack of response observed in mCRC patients treated with vemurafenib [73, 74]. Furthermore, B-RAF mutation in CRC patients is associated with low response rate against EGFR-targeted monotherapy [73, 77]. Cetuximab is a monoclonal antibody against EGFR and an established therapy for mCRC patients. In multiple studies *in vitro* and *in vivo*, vemurafenib was combined with cetuximab showing improved overall–and progression-free survival [69, 73, 74, 78]. These findings suggested a sustained antitumor activity and enhanced clinical outcome following vemurafenib in combination with EGFR-targeted therapy for the treatment of CRC patients [69, 73].

Recently, mutated B-RAF was reported found in several sarcoma subtypes, including liposarcoma cell lines [22], GIST patient tumors [79] and some tumors of clear cell sarcoma (CCS) patients [80-82]. This suggests that selected sarcomas should be further evaluated for a personalized medicine approach targeting B-RAF.

2 Aims of the study

The purpose of this study was to perform preclinical testing to evaluate whether therapies targeting the B-RAF^{V600E} mutation, also display efficacy against sarcomas with this mutation.

More specifically:

- ✓ Identifying sarcoma cell lines with the B-RAF^{V600E} mutation which could be used as *in vitro* models.

- ✓ Assess the efficacy of inhibitors targeting the B-RAF^{V600E} mutation, with regard to growth inhibition, cell death and cell cycle distribution.

3 Methods

This section describes the different methods that have been used in this study. A complete overview of materials including all solution, are listed in the appendices.

3.1 Mutation analysis of cell lines

The focus of this study was sarcoma cell lines with the B-RAF^{V600E} mutation. Thirteen liposarcoma cell lines have been sequenced in our laboratory. We examined the bam-files with raw sequencing data using the Integrative Genomics Viewer (IGV) software, to identify the mutation at the DNA level. Messenger RNA (mRNA) sequencing data were analyzed to validate the presence of mutation, and determine the level of expression. In order to normalize expression values based on the number of reads per sample and the length of the mRNA, we calculated reads per kilobase million (RPKM) values for each transcript. We found that two of the thirteen sequenced cell lines (SA-4 and SW872) express the B-RAF^{V600E} mutation We also data-mined the literature and searched in publically available databases, such as American Type Culture Collection (ATCC), to find additional sarcoma cell lines with the mutation. We identified a synovial sarcoma cell line (SW982) and a Ewing's sarcoma cell line (A673), both expressing the B-RAF^{V600E} mutation. The four sarcoma cell lines, which are all heterozygous for the mutation, were selected as models in the present study.

The two human melanoma cell lines, A375 and WM9, known to harbor the BRAF^{V600E} mutation, were included as positive controls. The A375 cell line is homozygous for the mutation, whereas WM9 is hemizygous. LPS510, characterized as a dedifferentiated liposarcoma (DDLPS) was established from a DDLPS tumor. This cell line lacks the B-RAF^{V600E} mutation and was used as a control cell lines not expected to respond to targeted treatment. All cell lines included in the study are listed in **Table 3.1**.

Table 3.1. Cell lines used in the present study.				
Cell line	**Tissue origin**	**Zygosity**	**BRAF-status**	**Provider**
A375	Human melanoma (metastatic)	Homozygous	V600E	ATCC
WM9	Human melanoma	Hemizygous	V600E	Rockland
LPS510*	Dedifferentiated liposarcoma	Homozygous		Dr. Fletcher, Harvard Medical School, Boston, USA
SA-4*	Liposarcoma	Heterozygous	V600E	ATCC
SW872*	Liposarcoma	Heterozygous	V600E	ATCC
A673	Ewings' sarcoma (muscle)	Heterozygous	V600E	ATCC
SW982	Synovial sarcoma	Heterozygous	V600E	ATCC

*Cell lines sequenced in our group at Section of Tumor Biology, Oslo University Hospital

3.2 Cell culturing and treatment

All cells were maintained in a 37 ºC humidified cell culture incubator with 5 % CO_2. The cells used in this study were adherent and grown in two-dimensional monolayer tissue-culture flasks and dishes (Sigma-Aldrich). All the cell lines were cultured in a complete growth media consisting of RPMI-1640 growth medium supplemented with 10 % fetal bovine serum (FBS) as well as 1 % L-alanine-L-glutamine (Glutamax™). Antibiotic (penicillin/streptomycin) was also included in the growth media.

Cells were passaged twice a week. When the cell culture had reached approximately 80 % confluence, media was removed and cells were washed with phosphate-buffered saline (PBS). Trypsin-EDTA (0.25% trypsin/0.03%) was added and cells were incubated for approximately five minutes to ensure complete detachment. An appropriate amount of fresh media was added for the deactivation of the trypsin. Slow growing cells were passaged 1:5 – 1:8, whereas a sub-cultivation ratio of 1:12 was used for the most rapid growing cell lines. All cell lines used in this study had been fingerprinted by short tandem repeat (STR) profiling to ensure correct identity of the cell stock. Furthermore, all cell lines were tested for mycoplasma infection using the Venor ® GeM Mycoplasma detection kit (Minerva Biolabs) for PCR.

Freezing and retrieval of cells

For storage, cell pellets were suspended in freezing media and approximately 10^6 cells were aliquoted in cryotubes and subsequently stored at -80 ˚C. After approximately three months of culturing, cells were substituted with a fresh stock.

Frozen cells were retrieved by briefly thawing the cells in a 37 ºC water bath. An appropriate amount of fresh growth media was added drop-wise, and the suspension was gently transferred to a 15 ml tube. Cells were further washed in PBS and centrifuged at 338 *g* for 5 minutes. The supernatant was removed and the cells were gently resuspended in pre-warmed growth media. The cells were subsequently transferred to a culture flask and placed in the incubator. The cells were passaged at least two times before they were used in experiments.

Drug treatment of cells

Live cells were counted with the automatic cell counter (Countess ®, Invitrogen) in the presence of trypan blue to exclude dead cells. Cells were seeded out at a concentration of 1000 – 3000 cells per well in 96 well plates and 10 000-500 000 cells in 6-well plates the day before experiments (the concentration is cell-line specific and depends on cell size and growth rate). Cells were treated either with the selective B-RAF^{V600E} inhibitor, PLX4032 (vemurafenib, Zelboraf) or RO5126766 (CH5126766) which is a pan-inhibitor with affinity to all RAF isoforms and their downstream kinase MEK1. Vemurafenib and RO5126766 were dissolved in dimethyl sulphoxide (DMSO) at a stock concentration of 10 mM and 1 mM, respectively. When used in experiments, the inhibitors were diluted in complete growth media in a final volume of 200 µl per well in 96-well plates and 2 ml in 6-well plates. To confirm that the cell growth was not affected by the DMSO, cells treated with DMSO only were included in all assays as a control.

3.3 Functional assays

A number of functional assays were performed to evaluate the preclinical efficacy of the selected inhibitors as therapeutics for B-RAF^{V600E} mutated sarcomas. The functional assays used measure

different cell characteristics such as cell growth, metabolic activity, apoptosis (by caspases-3/-7 activity) and cell cycle distribution.

3.3.1 Determination of cell growth by time-lapse microscopy

Cellular growth was measured by time-lapse microscopy, which allows continuous monitoring of the cells. The IncuCyte ZOOM or IncuCyte FLR systems (Essen BioScience) were used, which are fully automated microscopes with the same conditions as a standard cell incubator. A camera placed inside the incubator allows live-cell imaging with a pre-determined frequency (e.g. every 3 hours), providing high-definition phase-contrast images. The system's software calculates cell density based on the area of the well covered with cells, which generally correlates with cell growth. The system recognizes cells using a standard algorithm. However, due to heterogeneous morphology, the IncuCyte systems allow the operator to create a "mask" with defined parameters such as size, to ensure optimal detection of the cells.

Cells were placed in the IncuCyte systems when drug had been added, and monitored until approximately 100 % confluence was reached for the control-treated cells. Both cell growth curves and phase-contrast images showing cellular morphology were analyzed using the IncuCyte ZOOM and IncuCyte 2011A softwares.

3.3.2 CellTiter 96 ® AQ_{ueous} One Solution Cell Proliferation Assay (MTS assay)

The purpose of the MTS assay in this study was to evaluate the efficacy of the selected inhibitors by measuring the number of remaining viable cells quantitatively, after treatment. MTS is a colorimetric method based on the ability of metabolic enzymes in live cells, to reduce the MTS tetrazolium reagent to a colored formazan product.

Approximately after 72-120 hours of treatment with either inhibitor, MTS reagent (10 % v/v) was added to the cells, according to the manufacturer's instruction. The cells were incubated for up to two hours allowing the MTS reagent to be absorbed by the cells. A yellow-to-brown color change was observed following incubation which was measured by absorbance at 450 nm using the Modulus™ Microplate reader (Promega).

3.3.3 Apoptosis assay

Apoptosis is the process in which cells undergo programmed cell death, and is an essential feature to maintain tissue homeostasis. Apoptotic stimuli activate certain proteases called ”caspases” (cysteine aspartate proteinases), in particular caspases 3 and 7. Caspase-3/-7 are effector molecules and early markers of apoptosis, which can be activated by extrinsic or intrinsic signals. Upon stimuli, activated caspases-3/-7 binds to a specific recognition motif consisting of four amino acids (aspartate (D), glutamate (E), valine (V) and another aspartate (D) = DEVD).

Cells were seeded in triplets, in 96-well plates one day before treatment. Cells were treated with drug supplemented with the CellPlayer kinetic caspases-3/7 reagent (diluted 1:1000). The CellPlayer reagent consists of a DEVD motive bound to a DNA intercalating dye NucView™488 (=CellPlayer). Only in cells with activated caspases-3/-7, DEVD is cleaved which releases the DNA binding dye that translocate to the nucleus. Upon binding to DNA, the dye emits a green fluorescence that can be detected. The cells were monitored by time-lapse microscopy. A fluorescent metric was selected to detect caspases-3/-7 active cells after 72 hours, displayed as round, green fluorescent cells.

3.3.4 Cell cycle analysis

Cell cycle analysis by flow cytometry is an analytical method which can be used to distinguish the cells in different phases of the cell cycle, based on the content of DNA. The method is based on the transport of single cells in a suspension through a laser beam, thereby emitting a light. The data can be analyzed statistically, and cellular characteristics such as relative size, internal complexity of the cell and phenotype can be obtained.

3.3.4.1 Cell fixation and permeabilization

Ethanol was used to fix the cells and permeabilize the cell membranes, to allow the entry of the DNA-binding dye, Hoechst 33258, into the cell nuclei. Up to $1x10^6$ trypsinized cells were transferred to a 15 ml tube, washed twice with PBS and pelleted by centrifugation at 338 *g*. The cell pellet was then resuspended in an appropriate amount of PBS and vortexed while simultaneously pipetting ice-cold 96 % ethanol drop-wise to the tube (in a 1:5 ratio). The cells

were kept on ice during the experiment. The fixed cells were store at -20 ˚C for at least two hours, and potentially up to several months.

3.3.4.2 DNA detection

A variety of DNA dyes can be utilized for determining the cell cycle phases. The DNA dyes are stoichiometric, which means they bind in proportion to the amount of DNA present.

Fixed cells were pelleted by centrifugation at 939 *g* and washed with PBS twice before the cells were resuspended in 500 µl staining buffer. The cell suspension was filtered through a flow tube with a 70 µm mesh to remove cell aggregates, and up to $1x10^5$ cells were analyzed using the flow cytometry machine LSR II (BD Biosciences). Cells were detected with the UV laser (excitation 352 nm/emission 461 nm), and the FLOWJO v7.6.5 software was used to analyze the data. Forward scatter (measuring cell size) and side scatter (measuring intracellular complexity) were used to gate cells to ensure that only single cells were analyzed, and cell cycle histograms were obtained using the Watson setting.

3.4 Protein analysis by Western blotting

Western blot is an analytical method to detect and identify specific proteins in a cell sample. This method can separate proteins based on their molecular weight, electric charge, isoelectric point or a combination of these factors. In this study, sodium dodecyl sulphate polyacrylamide gel electrophoresis (SDS-PAGE) under reducing conditions was used to separate the proteins. SDS is a detergent that ensures uniform charge of the molecules and β-mercaptoethanol is a strong reducing agent which disrupts non-covalent bonds and linearizes the proteins. This method allows separation of proteins in an electric field based on their molecular weight.

3.4.1 Protein extraction

1x Lysis buffer was prepared by diluting 3x Lysis buffer, 7x protease inhibitors and 10x phosphatase inhibitors in PBS. Cells were washed twice with PBS and lysed in 1x Lysis buffer, boiled at 95 ºC for 10 min and centrifuged at 14000 *g* for 10 min. Samples were stored at -20 ºC to avoid protein degradation.

3.4.2 Determination of protein concentration

The protein concentration in the cell lysate was determined using the colorimetric Bio-Rad protein assay, a procedure based on the Bradford method. This method involves the binding of the acidic solution Coomassie brilliant Blue G-250 to proteins which induces a change in color. Intensity of color in the solution is proportional to the protein content in the sample, and can be measured by absorbance at 600 nm.

A relative standard curve was made consisting of five dilutions of bovine serum albumin (BSA) in protein assay dye (diluted 1:15 in water before use). In order to compensate for any interference effects of SDS present in the total protein lysates, an equivalent amount of 1x Lysis buffer was also added to the BSA standards. Total protein lysates were diluted 1:1000 in protein assay dye. Both the BSA standards and total protein lysates were incubated for 5 minutes and 200 µl were transferred in doublets to a 96-well plate. The Modulus™ Microplate (Promega) reader was used to measure the absorbance at 600 nm. The absorbance values obtained from the BSA samples were plotted in the formula "y=ax+b", and a standard curve was made with protein concentration on the x-axis and absorbance on the y-axis. The protein concentrations in the cell samples were calculated by comparing to the standard curve.

3.4.3 SDS-PAGE

LDS sample buffer was added to the cell lysates and incubated at 95 ºC for 10 min. A NuPAGE Bis-Tris 4-12 % gel and MOPS running buffer was used to separate the proteins, MOPS being the most effective running buffer for optimal separation of the proteins of interest. The wells were pre-washed with running buffer. 15 µg of total protein lysates were loaded per well. A protein standard was included to determine the molecular weight. The gel was set to run for 1.5-2 hours at 100 V on ice.

3.4.4 Gel transfer and blotting

After separation, the proteins were transferred from the gel to a polyvinylidene difluoride (PVDF) membrane. The membrane was pre-wetted in 100 % methanol to allow binding of proteins to the membrane. A transfer cassette was prepared in the following order: sponge pad, filter paper, the gel with the proteins, activated PVDF membrane, filter paper and sponge pad, all wetted in transfer buffer. Using a 1 x transfer buffer, the electrophoresis was set to run at 400

mA for one hour, on ice. After electrophoresis, the membrane was dried at room temperature (RT).

3.4.5 Antibody incubation and immunodetection

In this study chemiluminescense was used to detect the protein expression in the samples. Here we used a primary antibody to bind the protein of interest and a secondary antibody that recognizes the primary antibody. The secondary antibody is conjugated to Horseradish peroxidase (HRP) enzyme. Upon incubation in a "development solution" containing a substrate for HRP, the enzyme is activated which creates a luminescence activity that can be captured on film or by camera. The signal intensity correlates to the amount of proteins in the samples.

To reduce non-specific binding of the antibodies during protein detection, the pre-dried membrane was blocked with blocking buffer (either 10 % BSA or 10 % non-fat dry milk dissolved in TBS-T) for one hour at RT with shaking. The blocked membrane was further incubated in blocking buffer containing primary antibody at 4 ºC overnight while shaking. The membrane was washed with washing buffer three times á 5 min, and incubated in blocking buffer containing secondary antibody for 1 hour at RT while shaking. After antibody incubation, the washing procedure was repeated. The membrane was then incubated in a development solution for 5 minutes at RT while shaking before being placed in the digital developer G:BOX (Syngene). The digital developer detects the emitted signal and captures images which can be analyzed by the GeneSnap software.

3.5 Statistical analysis

The data obtained in this study were statistically analyzed using the Microsoft *Excel* software. A 2-tailed paired Student's t-test, measuring a data set with normal distribution, was used to compare the read-out of drug-treated with control-treated cells.

To calculate confidence of the MTS data, standard deviation (SD) was calculated between biological replicates, whereas for growth curves standard error of mean (SEM) was calculated. Both SD and SEM are illustrated by error bars.

4 Results

4.1 Expression of B-RAF^{V600E} mutation in sarcoma cell lines

The presence of B-RAF^{V600E} mutation has been reported in sarcomas [22]. In this study we have performed first stage preclinical testing of drugs targeting B-RAF^{V600E} in established sarcoma cell lines. First, we identified sarcoma cell lines with the mutation, to be used as model systems. Messenger RNA sequencing data available in our laboratory were examined for a number of cell lines. Two out of thirteen liposarcoma cell lines, SA-4 and SW872, were found to harbor the B-RAF^{V600E} mutation at the mRNA level consistent with a previous report [22]. We also searched publicly available databases, such as ATCC, to find additional sarcoma cell lines expressing the B-RAF^{V600E} mutation. Here we found that the A673 and SW982 cell lines derived from tumors characterized as Ewing and synovial sarcoma, respectively, both carried this mutation.

Two human melanoma cell lines (A375 and WM9) known to express the B-RAF^{V600E} mutation, were included as positive controls. A375 is homozygous for the B-RAF^{V600E} mutation, whereas WM9 is hemizygous (the wild-type allele is lost and the other allele is mutated). The dedifferentiated liposarcoma cell line LPS510, which did not harbor the B-RAF mutation, was included in the study as a control cell line not expected to respond to targeted therapy against B-RAF^{V600E}. The status of mutation at mRNA level for the cell lines used in this study is listed in **Table 4.1**.

As the sequencing data only provides information about the presence of a specific mutation at the RNA level, expression of mutated B-RAF^{V600E} was also validated at the protein level in all the cell lines. Cells were lysed and proteins were separated by SDS-PAGE, and subsequently analyzed by immunoblotting using two antibodies that bind either B-RAF^{V600E} or all variants of B-RAF (total B-RAF). Both B-RAF^{V600E} and B-RAF^{WT} have a molecular weight of 84 kDa (**Figure 4.1**). The B-RAF^{V600E} mutated protein was present in all cell lines except LPS510, and total B-RAF was abundant in all cells including LPS510. An antibody against α-tubulin was included as a protein loading control with an expected molecular weight of 50 kDa.

Table 4.1. Overview of cell lines used in the present study.					
Cell line	**Histology**	**Zygosity V600E B-RAF**	**% V600E**	**Provider**	**Reference**
A375	Melanoma	Homozygous	100	ATCC	ATCC
WM9	Melanoma	Hemizygous	100	Rockland	Rockland
LPS510	Dedifferentiated Liposarcoma		0	Dr. J. Fletcher (Harvard Medical School, Boston, USA)	*
SA-4	Liposarcoma	Heterozygous	48	ATCC	[22]*
SW872	Liposarcoma	Heterozygous	51	ATCC	[22]*
A673	Ewing's sarcoma	Heterozygous	N.D	ATCC	
SW982	Synovial sarcoma	Heterozygous	N.D	ATCC	

(*) Cell lines mRNA-sequenced in our laboratory. N.D: not detected.

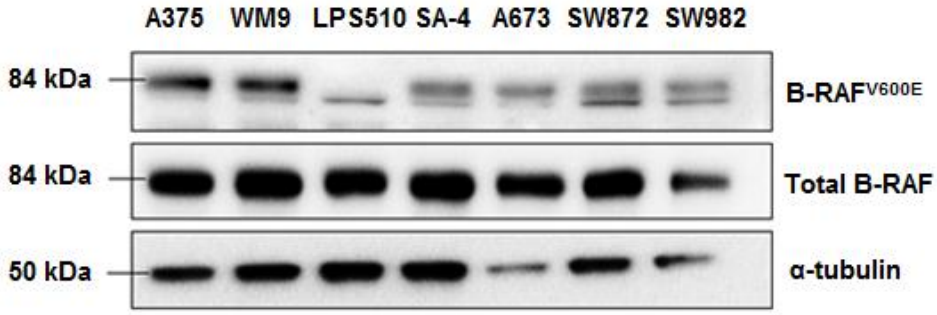

Figure 4.1: Protein expression of mutated B-RAF^{V600E} and total B-RAF. Western blot showing endogenous expression of B-RAF^{V600E} and total B-RAF, as indicated. The α-tubulin is included as a protein loading control. Note the unspecific band below the expected size in the B-RAF^{V600E} immunoblot.

4.2 Evaluation of vemurafenib efficacy on cell growth

As mentioned earlier, vemurafenib is a small molecule inhibitor specifically targeting B-RAF with the V600E mutation, approved by FDA for treatment of malignant melanoma. We wanted to investigate the effect of vemurafenib in the four sarcoma cell lines harboring the B-RAF^{V600E} mutation, to evaluate the potential of repurposing vemurafenib as targeted therapy for selected

sarcoma patients. All cell lines included in the study where treated with vemurafenib (40 nM-10 µM), and analyzed by MTS assay which estimates the amount of viable cells per well. The MTS assay was performed when the control cells (only treated with DMSO equivalent to the highest drug dose), had grown to ≈ 100 % cell confluence. For the melanoma cell lines, a dose-response was observed following treatment with vemurafenib (**Figure 4.2**)**.** The LPS510 cell line was unaffected up to 5 µM, which was expected since this cell line only has the B-RAF^{WT}. However, a minor effect was observed for LPS510 when treated with 10 µM of vemurafenib indicating an off-target response, perhaps through the B-RAF^{WT} protein or another kinase. For SA-4 and SW982, a dose-dependent reduction in the number of live cells was observed following vemurafenib treatment, although a significant response was only observed for the SA-4 cell line. In general, both SA-4 and SW982 cells required higher concentrations of vemurafenib than the melanoma cell lines. For A673, a reduction in cell number was observed already at 0.16 µM, but not in a dose-dependent manner. For SW872, a slight growth inhibition was observed for the highest concentrations of vemurafenib.

We also investigated the effect of vemurafenib (up to 5 µM) for all the cell lines by measuring cell growth using time-lapse microscopy (**Figure 4.3**). A375 and WM9 responded with a growth inhibition in a dose-dependent manner following treatment with vemurafenib, whereas for LPS510 no effect on cell growth was observed at any tested concentrations. For both SA-4 and SW982, a dose-dependent reduction in cell growth was observed in response to vemurafenib, similar to the growth inhibition observed for the melanoma cell lines. For A673, a reduction in cell growth was observed already at 0.16 µM, but no dose-response. For the SW872 cells, a minor growth reduction was observed following treatment.

Since morphological changes can affect cell density, we also performed a visual inspection of all the cell lines following treatment with vemurafenib. Images of the cells were examined and the number of cells was evaluated. For each cell line, a representative phase-contrast image is shown following treatment with vemurafenib (0.63 and 5 µM) and control-treated cells for 72 hours (**Figure 4.4**). The control-treated melanoma cell lines were characterized by the typical cobblestone morphology where cells are in close contact with each other, resembling epithelial cells. However, upon treatment with vemurafenib, A375 cells changed morphologically appearing elongated. For both melanoma cell lines, a reduced number of cells were observed

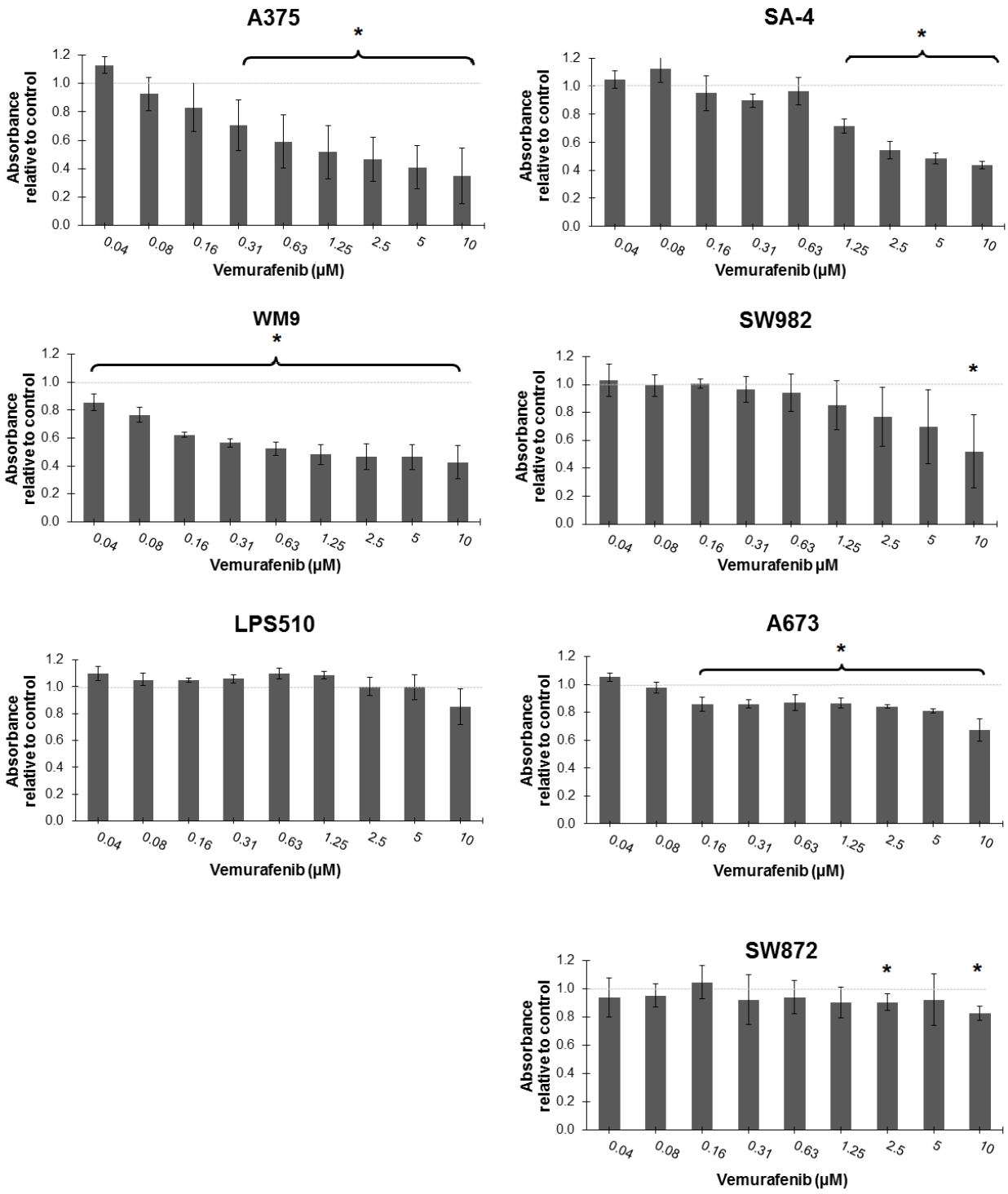

Figure 4.2. Effect on cell growth after treatment with vemurafenib. After 72 hours of treatment for the control cell lines and up to 120 hours for the sarcoma cell line with the indicated concentrations of vemurafenib, cell growth was estimated by MTS analysis. The absorbance 450 nm was measured and normalized to control-treated cells (DMSO corresponding to the highest concentration of drug). Columns represent mean of three biological experiments and error bars represent standard deviations (n=3). (*) indicates statistical significance measured by a two-tailed, paired t-test (*=$p \leq 0.05$).

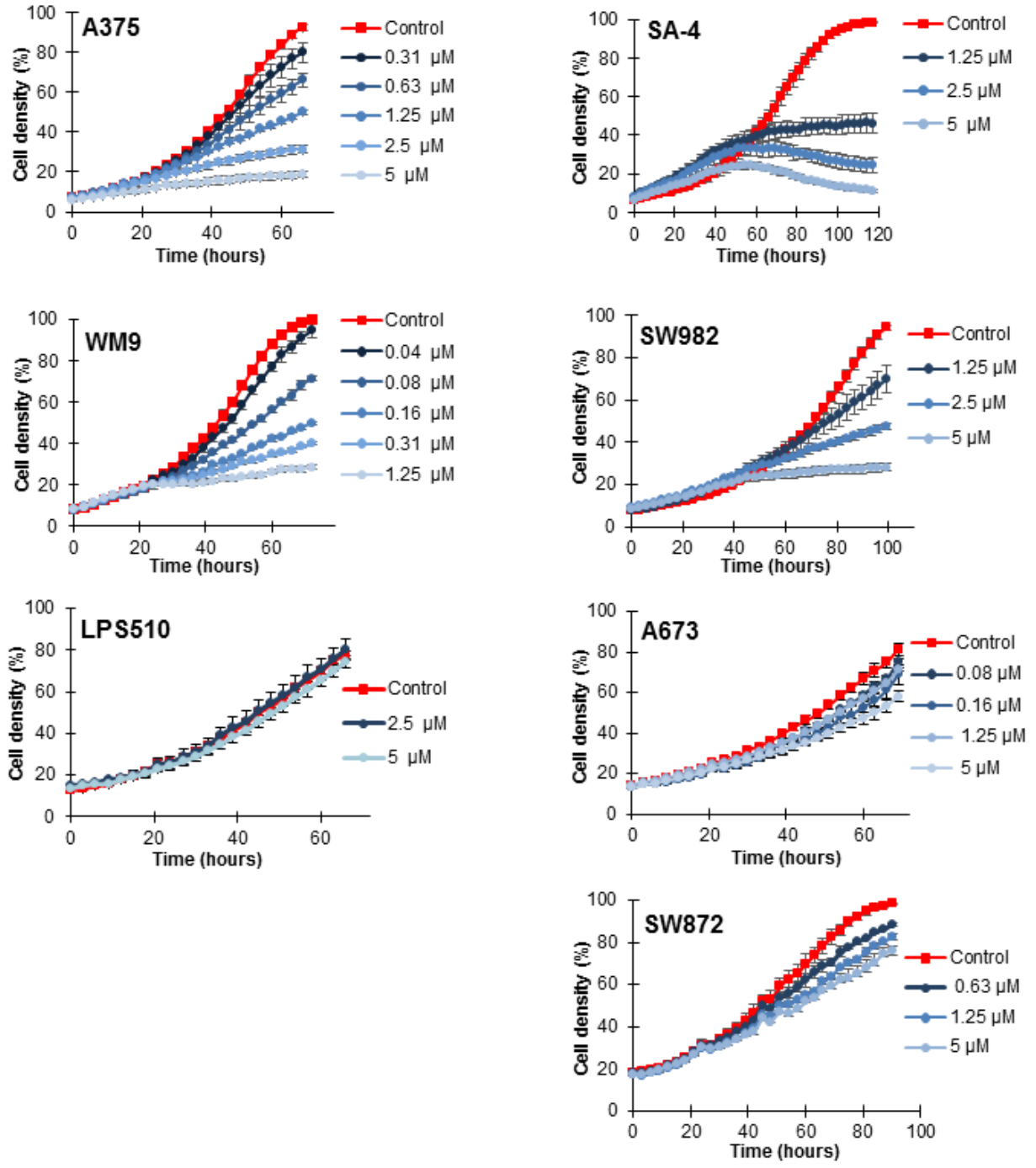

Figure 4.3. Growth rate of cells treated with vemurafenib. Cell density was monitored by time-lapse microscopy during treatment with the indicated concentrations of vemurafenib or control (DMSO corresponding to the highest drug concentration). One representative experiment is shown for each cell line (n=3). The error bars represent standard error of mean (SEM) between technical replicates.

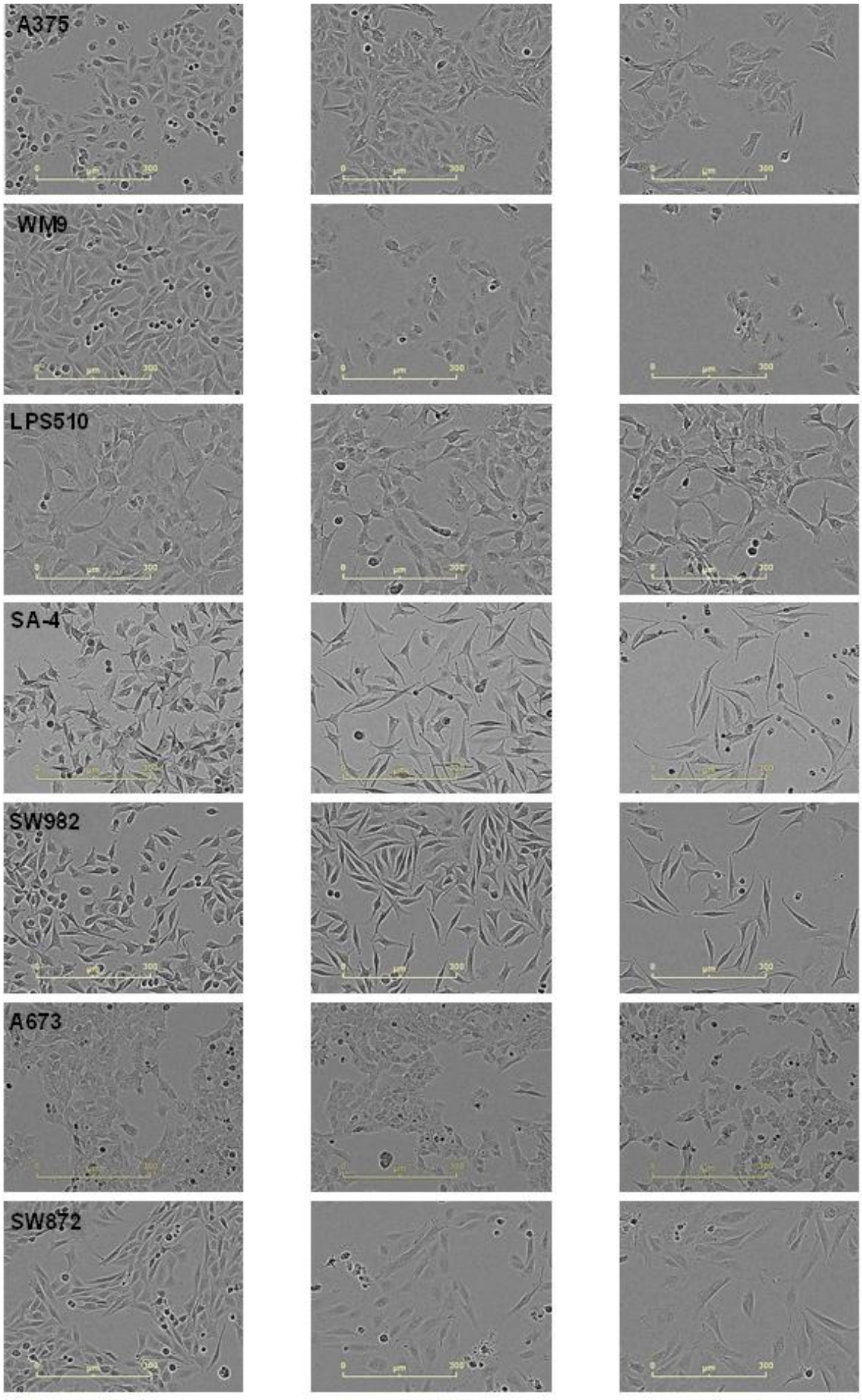
A375
WM9
LPS510
SA-4
SW982
A673
SW872
Control
0.63 µM
5 µM

Figure 4.4. Morphological changes of cells upon treatment with vemurafenib. Cells were treated with indicated dose of vemurafenib or control (DMSO corresponding to the highest drug concentration). Representative phase-contrast images (taken with the 10x objective microscope in the IncuCyte ZOOM) are shown after 72 hours.

compared to the control-treated cells, indicating reduction in cell growth. Untreated LPS510 cells appeared elongated and fibroblastic. This cell line, lacking the B-RAF^{V600E} mutation, did not undergo morphological changes upon treatment with vemurafenib. Moreover, no apparent change in confluence was observed independent of treatment. Untreated SA-4 and SW982 cells appeared "triangular" in morphology. However, upon treatment with vemurafenib, a major change in morphology was observed for SA-4 cells, which acquired a shape resembling long, thin spindle-shaped fibroblastic cells with some cells appearing "star-shaped". Also the SW982 cells became "outstretched" following treatment, although to a lesser extent. A reduction in cell number was observed for both SA-4 and SW982 following treatment with 5 µM of vemurafenib (a reduced cell number was also observed for SA-4 cells treated with 0.63 µM). A673 control cells were characterized by their cobblestone-morphology. Upon treatment with vemurafenib, no change was observed in either cellular morphology or cell confluence. Untreated SW872 cells appeared as long cells growing in close contact with each other. Upon treatment, the cells changed morphologically and appeared larger and more "outstretched". The phase-contrast of SW872 cells was greatly reduced following treatment, making it more challenging to detect the cells. A minor reduction in cell number was observed following treatment of SW872 cells.

In summary, the melanoma cell lines responded well to vemurafenib, as demonstrated by both the MTS assay and time-lapse microscopy. A reduction in cell number was also observed following treatment. LPS510, which lacks the B-RAF^{V600E} mutation, did not respond to treatment with vemurafenib, as expected. In general, for the sarcoma cell lines expressing the mutations, the results from the two assays corresponded. The greatest response to vemurafenib was seen for SA-4 cell upon treatment with the inhibitor, at concentrations ranging from 1.25 to 5 µM.

4.3 Vemurafenib induces apoptosis and cell cycle arrest in SA-4 cells

Since SA-4 was the sarcoma cell line with the greatest response to vemurafenib treatment, we wanted to further characterize these cells to understand the underlying cause of the growth inhibition following treatment. First, the induction of apoptosis was investigated following treatment of SA-4 cells with 2.5 or 5 µM vemurafenib in the presence of the CellPlayer reagent. The reagent couples the recognition motif for activated caspase-3/-7 to an intercalating DNA dye. Activated caspases-3/-7 cleaves the binding between the recognition motif and the dye, which enables the dye to enter the nucleus and bind to DNA, and thereby emit a green fluorescence. The fluorescence can be detected and measured by absorbance at 488 nm. The cells were monitored by time-lapse microscopy for 72 hours.

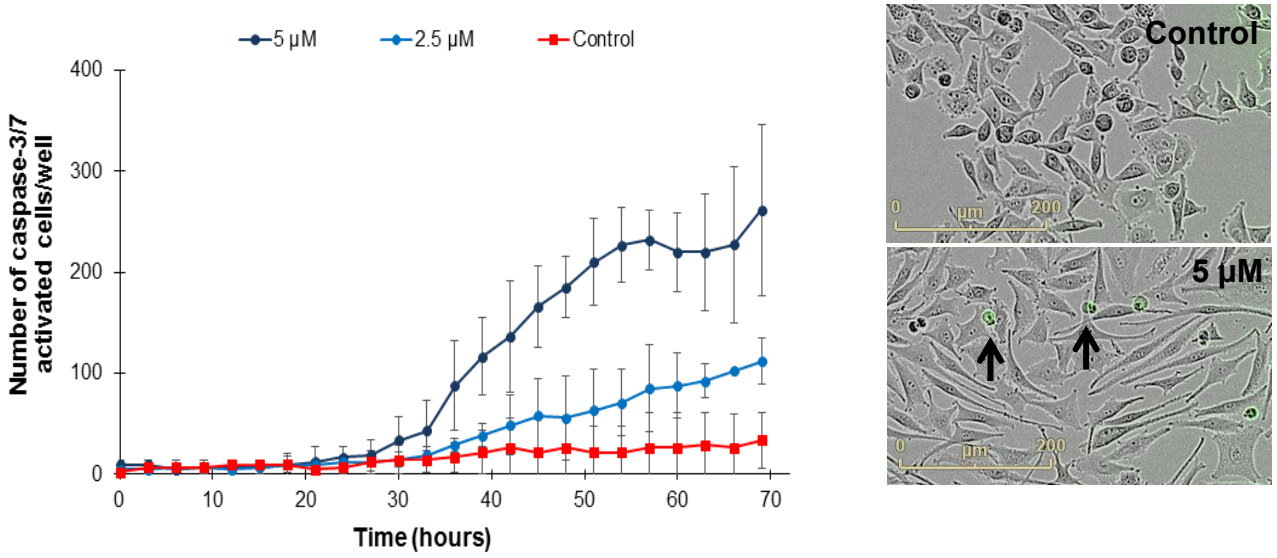

Figure 4.5. Caspase-3/-7 activity in SA-4 cells treated with vemurafenib. **A)** Apoptotic cells were determined based on caspases-3/-7 activity measured by time-lapse microscopy, during treatment with 2.5 or 5 µM vemurafenib or control (DMSO corresponding to the highest concentration of drug) supplemented with the CellPlayer reagent. The curve displays the number of caspases-3/-7 active cells per well over time. The curve from one representative experiment is shown (n=3). Error bars represent the standard error of mean (SEM) between technical replicates. **B)** Representative images of SA-4 cells treated with 5 µM vemurafenib and control-treatment after 50 hours are shown (displaying phase-contrast and fluorescence at 488 nm). Caspase-3/-7 active cells (shown as green cells rounded up) are indicated by the black arrows.

A dose-dependent induction of apoptosis was observed following treatment of SA-4 cells with vemurafenib, shown as an increased number of caspases-3/-7 activate cells (**Figure 4.5 A**). In addition, the presence of apoptotic cells was verified by visual inspection of green fluorescence-images from the experiment (**Figure 4.5 B**). However, only a subset of SA-4 cells underwent apoptosis upon treatment with vemurafenib, and viable cells were also present following treatment with the highest concentration (5 µM). We therefore investigated the effect of vemurafenib on cell cycle progression.

SA-4 cells were treated with 0.31 and 1.25 µM of vemurafenib for 48 hours, fixed and permeabilized with ethanol and stained with the DNA-binding dye Hoechst 33258. The dye binds in a stoichiometric fashion, meaning it represents the amount of DNA present. Subsequently, cell cycle analysis was performed by flow cytometry showing the distribution of cells in the different phases of cell cycle (**Figure 4.6**). Sub-G_1 (referring to a cell population with less amount of DNA than expected for cells in G_0/G_1) is also included. The FLOWJO software was used to analyze the cell cycle data. An increased number of cells were observed in G_0/G_1-phase (cells "resting" or preparing for division) upon treatment with vemurafenib compared to the control-treated cells. Furthermore, a higher number of cells were detected in G_0/G_1-phase following treatment with 1.25 µM compared to 0.31 µM. The number of cells in S-phase (DNA replication) was decreased in a dose-dependent manner. A reduced number of SA-4 cells were in G_2-phase (cell growth and preparing for division) when treated with 0.31 µM vemurafenib compared to the control-treated cells. For cells exposed to 1.25 µM, a highly reduced number of cells were detected in G_2-phase, indicating an arrest in G_1. An increased population of cells in Sub-G_1 was detected following vemurafenib treatment, which is typical for necrotic or early apoptotic cells.

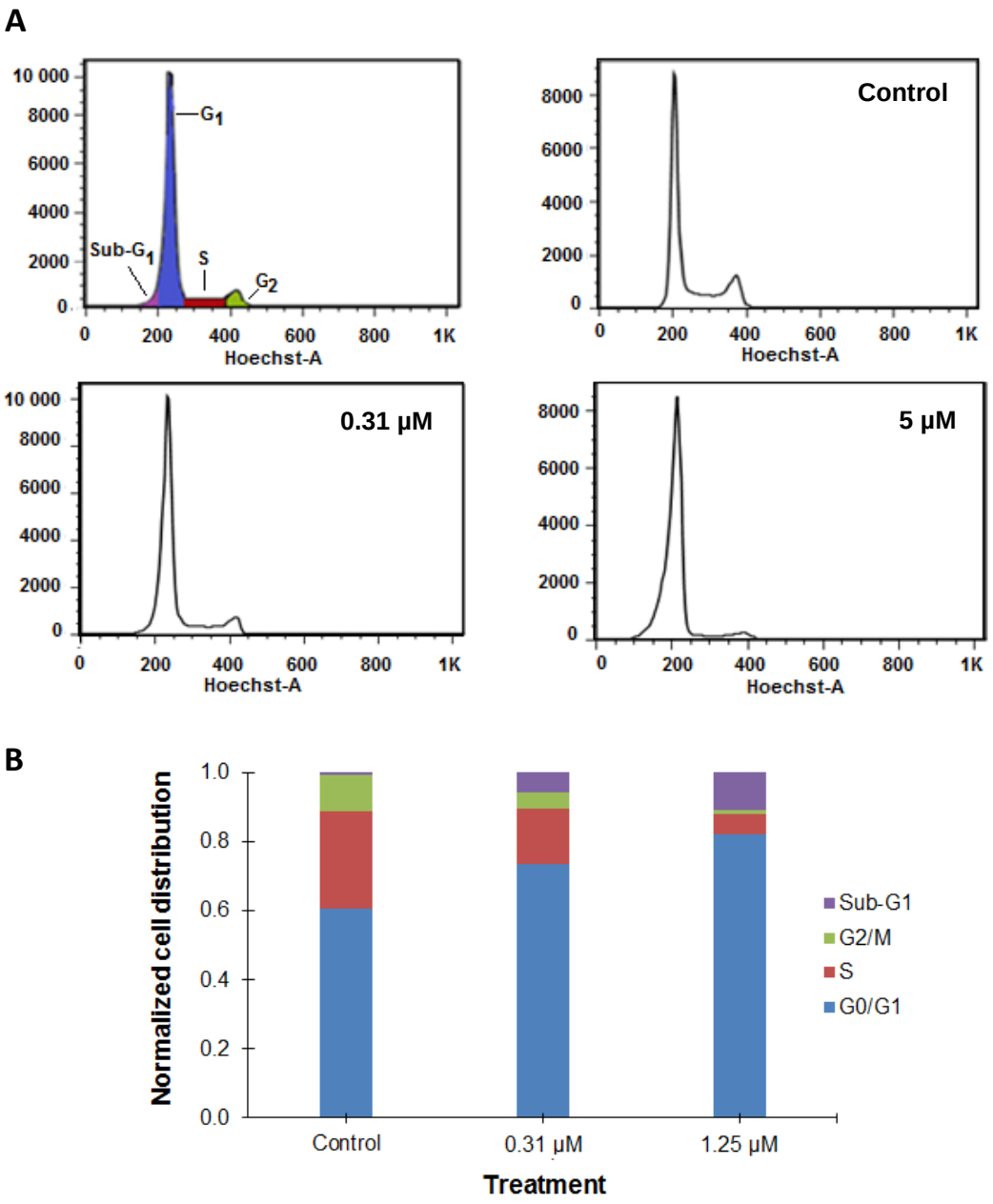

Figure 4.6. Cell cycle distribution of SA-4 cells treated with vemurafenib. Cells were treated with the indicated concentrations of vemurafenib or control (DMSO corresponding to the highest concentration of vemurafenib) for 48 hours, and analyzed by flow cytometry. The data were analyzed by the FLOWJO software. **A)** A representative histogram is shown for each treatment (n=3). The y-axis represents the number of cells and the x-axis shows the relative amount of DNA. The 0.31 µM-treated sample (indicated by colors) is used to demonstrate the phases of cell cycle. **B)** Representative bars illustrating the cell distribution among the phases of cell cycle. The data are normalized to control, and sub-G1 is included to complete cell cycle distribution values.

Based on these experiments, cell cycle arrest appeared to be the major contributing factor to the growth inhibitory effect of vemurafenib in SA-4 cells.

4.4 Vemurafenib induces a reversible inhibitory effect in SA-4 cells

It has been reported in melanomas that there is a need for continuous treatment of melanoma patients with vemurafenib. Thus, we also investigated the consequence of removing the drug during cell growth, to see if the observed growth arrest was reversible. SA-4 cells were exposed to 1.25, 2.5 or 5 µM vemurafenib and the cells were monitored by time-lapse microscopy up to 500 hours. The drug was removed after 120 h, 240 h or 310 h of treatment and replaced by fresh growth medium without vemurafenib.

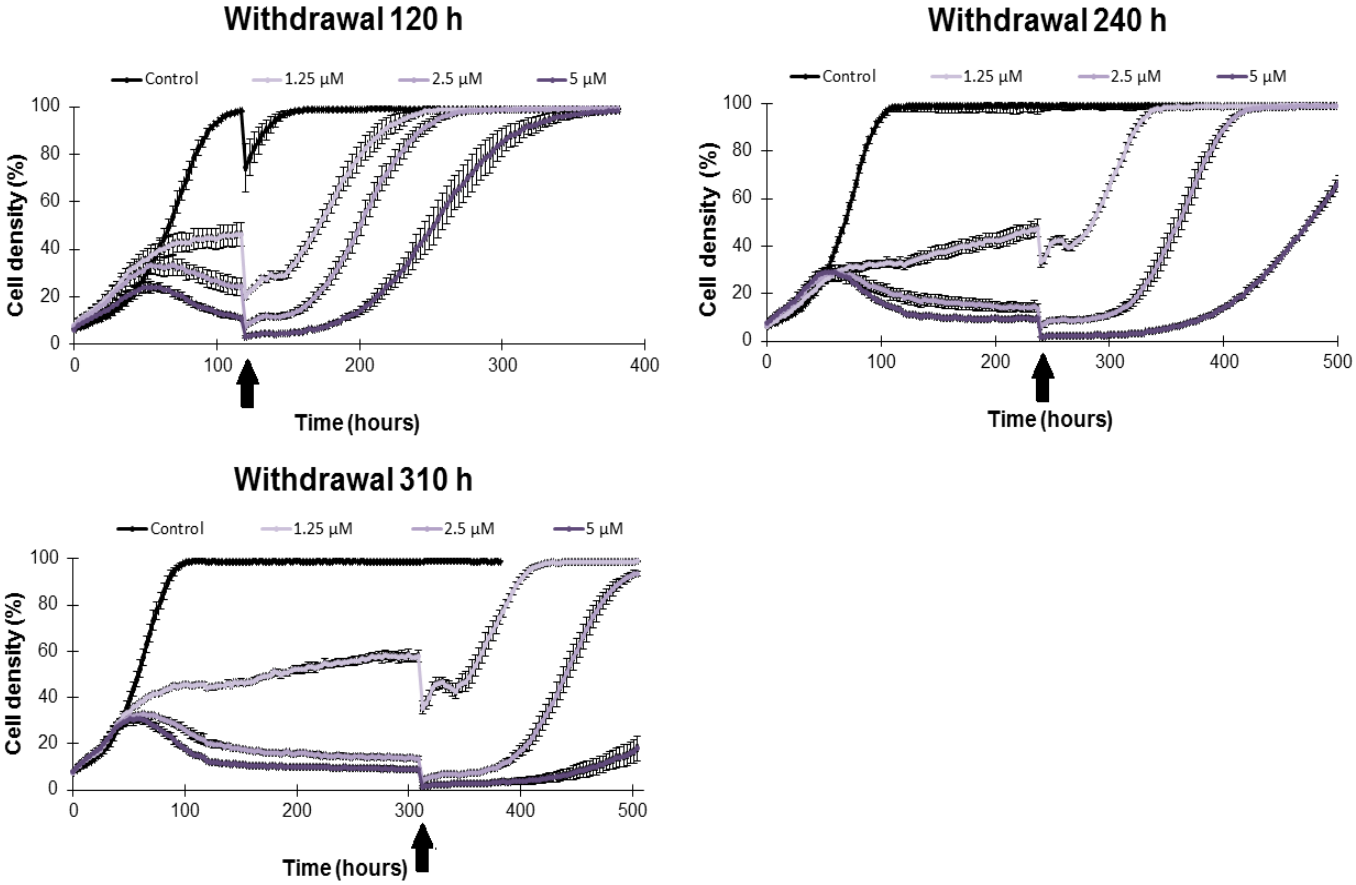

Figure 4.6: Growth of SA-4 cells after removal of vemurafenib. SA-4 cells were treated with the indicated concentrations of vemurafenib and control (DMSO corresponding to the highest drug concentration) over an extended period. Growth medium supplemented with vemurafenib was withdrawn at specific time points (indicated by a black arrow) and replaced with regular growth medium. Cell growth was monitored by time-lapse microscopy. Growth curves from one representative experiment is shown (n=2). Error bars represent standard error of mean (SEM) between triplicates.

SA-4 cells resumed cell growth upon removal of drug, independent of the drug concentration or duration of treatment. Cells exposed to 5 µM vemurafenib needed longer recovery time to resume cell growth. This could partly be due to a reduced cell confluence, which affects the growth rate. However, the fact that the cells were able to resume growth suggests that vemurafenib exerts a temporary growth inhibition and that the effect is reversible upon removal.

To validate the results, a visual inspection of cells from before and after removal of vemurafenib was also performed by examining phase-contrast images (**Figure 4.7**). Although the majority of cells were dead at the time of drug removal, resumed cell growth was observed for a subset of the living cells after drug withdrawal, demonstrating that these cells had the capacity to grow and divide again when inhibitor was removed.

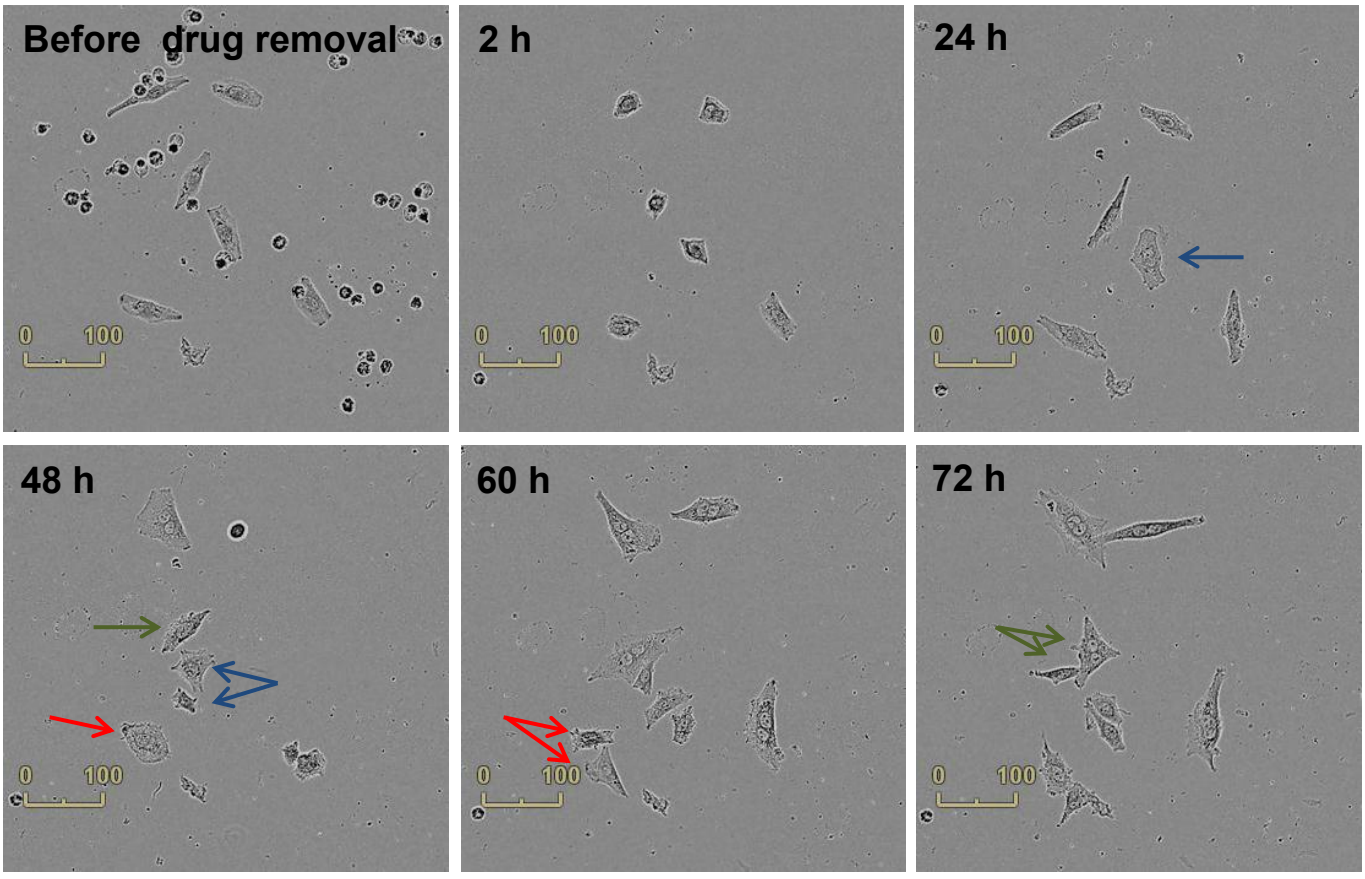

Figure 4.7. Cell growth of SA-4 cells after removal of vemurafenib. Cells treated with 5 µM vemurafenib were monitored by time-lapse microscopy (using 10x objectives in IncuCyte). Representative phase-contrast images of the same field are shown before and at the indicated hours of recovery after drug removal. Colored arrows indicate cells before and after cell division. For example, the blue arrow at 24 hours of recovery after drug removal indicates a cell that is in division and by 48 hours has divided into two daughter cells (indicated by two blue arrows).

Since the effect of vemurafenib appeared reversible in the best responding cell line SA-4, we wanted to test another therapeutic strategy.

4.5 Evaluating efficacy of RAF/MEK1 dual inhibitor as therapy for B-RAF^{V600E} mutated sarcomas

Both RAF and MEK kinases activate ERK kinase, which is a main transmitter of growth signals into the nucleus thereby stimulating cell growth. Since the effect of vemurafenib was reversible in SA-4 cells, we wanted to test other inhibitors targeting B-RAF^{V600E} in our cell models. A dual inhibitor, RO5126766, targeting both RAF and its downstream kinase MEK1 is currently in clinical trials [83, 84]. We therefore compared the efficacy of RO5126766 and vemurafenib on the phosphorylation of ERK in the four sarcoma cell lines. Cells were treated with 5 µM vemurafenib, 300 nM RO5126766 or control (with DMSO) for 3 hours, and protein lysates were subsequently analyzed by immunoblotting. The selected concentrations of RO5126766 used for the immunoblotting analysis and in subsequent experiments were based on previous experiments performed within the Myklebost group.

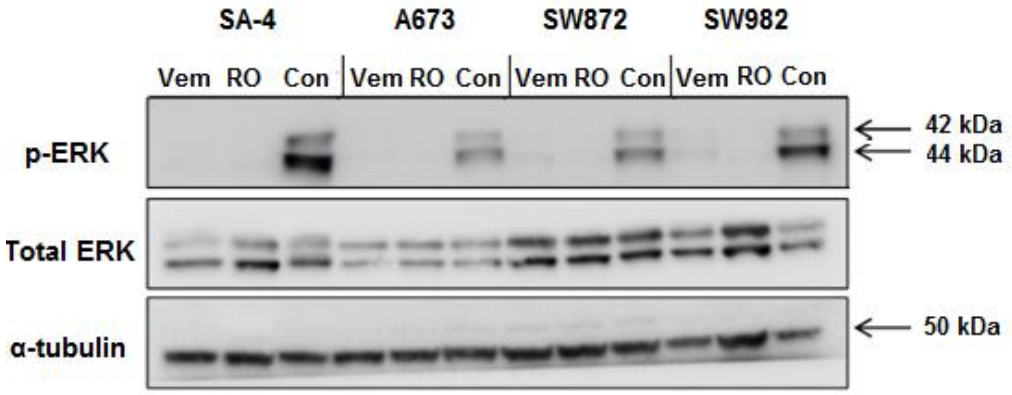

Figure 4.8. Protein expression of p-ERK in sarcoma cell lines treated with vemurafenib or RO5126766. Sarcoma cell lines were treated with either 5 µM vemurafenib (Vem), 300 nM RO5126766 (RO) or control (Ctr; with DMSO) for 3 hours. Protein expression was evaluated by immunoblotting, using the indicated antibodies, p-ERK and total ERK (with molecular weights of 42/44 kDa). Antibody against α-tubulin was included as a protein loading control (with a molecular weight of 50 kDa).

Immunoblotting with an antibody against total-ERK confirmed the presence of ERK protein in all cell lines independent of treatment (**Figure 4.8**). Immunoblotting with an antibody against p-ERK showed that all the four sarcoma cell lines had phosphorylated ERK endogenously. When comparing the effect of vemurafenib and RO5126766 on the phosphorylation of ERK, a strong reduction in the expression of p-ERK was observed for all the four sarcoma cell lines following treatment with either inhibitor. This indicated that both vemurafenib and RO5126766 inhibit ERK phosphorylation successfully in all the tested cell lines.

As RO5126766 successfully suppressed the expression of p-ERK at the protein level, we investigated the efficacy of the inhibitor on cell growth. The four sarcoma cell lines and the control cell line LPS510 (without the B-RAF^{V600E} mutation) were treated with RO5126766 (100-400 nM) up to 100 hours and analyzed by MTS assay. A dose-dependent reduction in cell growth was observed in SA-4 and SW982 following RO5126766 treatment (**Figure 4.9**). However, the most significant effect was observed following treatment of SA-4 cells for all the tested concentrations. For A673 and SW872, a minor response was observed following treatment. LPS510 did not respond to treatment with RO5126766. In fact, instead a paradoxical increase in cell growth was observed.

The effect of RO5126766 on cell growth was also investigated using time-lapse microscopy (**Figure 4.10**). A dose-dependent reduction in cell growth was observed for SA-4 and SW982 cells following treatment with RO5126766. For A673 and SW872, a minor response was observed following treatment.

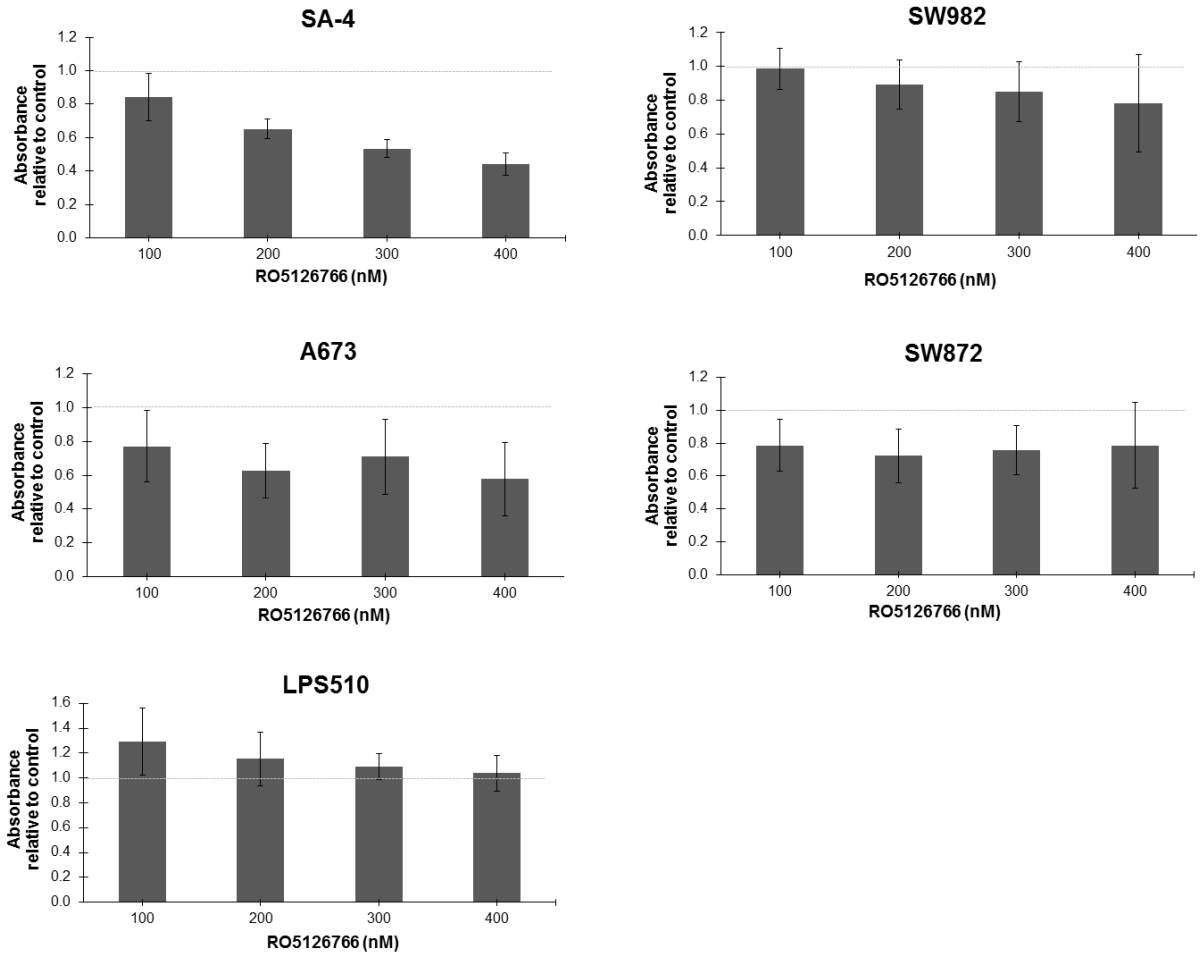

Figure 4.9: Cell growth after treatment with RO5126766. After approximately 100 hours of treatment for SA-4, A673, SW872 and SW982, and 120 hours for LPS510 with the indicated concentrations of RO5126766, cell growth was estimated by MTS analysis. The absorbance at 450 nm was measured and normalized to control (DMSO corresponding to the highest concentration of drug). Columns represent mean of three biological experiments and error bars represent standard deviations (n=3). (*) indicates statistical significance measured by a two-tailed, paired t-test (*=$p \leq 0.05$).

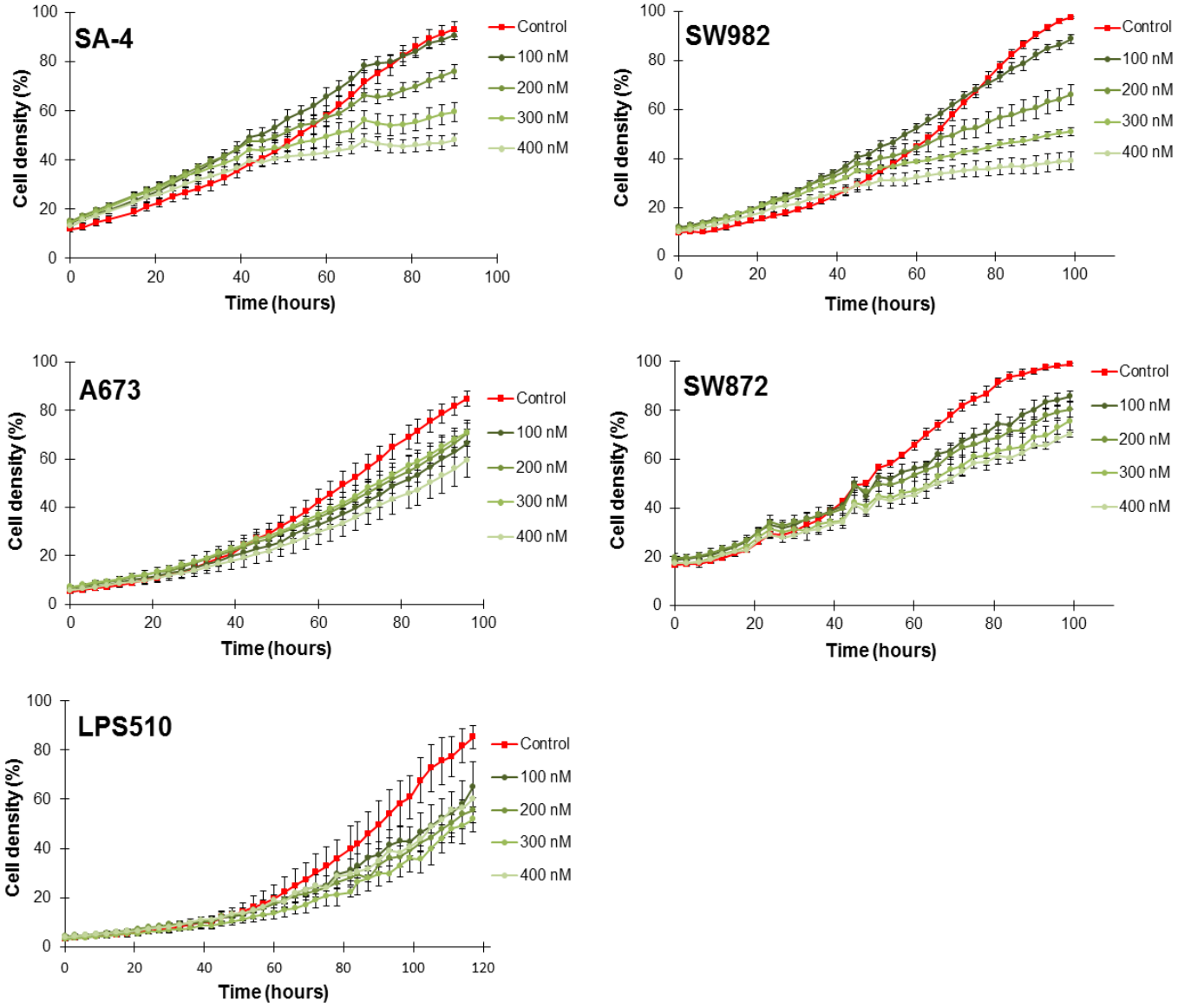

Figur 4.10: Growth rate of cells treated with RO5126766. Cell density was monitored by time-lapse microscopy during treatment with the indicated concentrations of RO5126766 or control (with DMSO corresponding to the highest drug concentration). One representative experiment is shown for each cell line (n=3). The error bars represent the standard error of mean (SEM) between technical triplets.

In summary, inhibition of ERK phosphorylation was observed for all the four sarcoma cell lines following treatment with either vemurafenib or RO5126766. However, cell growth analysis revealed a greater growth inhibitory response for SA-4 and SW982 cells following treatment with RO5126766, compared to A673 and SW872 cells**.**

5 Discussion

The B-RAF^{V600E} mutation has been described in several sarcomas [22]. In this study, we aimed to treat sarcoma cells which have the B-RAF^{V600E} mutation, either with vemurafenib (specifically targeting B-RAF^{V600E}) or RO5126766 (which targets both B-RAF and its downstream signaling molecule MEK). Sarcoma cell models were identified with regard to mutational status, and selected accordingly. The most significant inhibitory effect was observed for SA-4 cells following treatment with either of the inhibitors. SA-4 cells were further investigated with regard to cell death and cell cycle progression following treatment with vemurafenib. Short term treatment with the inhibitor induced apoptosis in a small fraction of SA-4 cells and a G_1-arrest in a larger amount of the cells. However, the SA-4 cells were able to resume growth following removal of vemurafenib, indicating a reversible effect of the inhibitor and a need for continuous treatment. The SW982 cell responded to vemurafenib treatment, although the growth inhibition was not significant. For the remaining two cell lines, SW872 and A673, a minor growth inhibition was observed following treatment with either vemurafenib or RO5126766.

5.1 Methodological considerations

Normally, preclinical testing of novel drugs involves testing of efficacy *in vitro* using cell lines and *in vivo* using animal models. In cancer research, human cancer cell lines are frequently used as model systems as they have retained hallmarks of cancer [85]. Human cancer cell lines harbor characteristics of the tumor it was derived from and are considered to be useful models, making them eligible for use in cancer research. However, the genetics and epigenetics of cancer cell lines may differ from cells in *in vivo* tumors. Furthermore, within the tumor, cancer cells live in a microenvironment with other tumor cells as well as normal cells, forming clones and competing for space and nutrients, a condition not present *in vitro*. Two-dimensional cell cultures (which are used in this study) are valuable in certain aspects of experimental work. However, *in vivo* models such as xenograft models (human tumors engrafted in immunocompromised mice) more closely resemble the tumor in patients. Such *in vivo* models, which are used in the second stage

of preclinical testing, are considered to be more attractive for preclinical assessment of drug efficacy [86, 87].

Several factors may complicate the use of human cancer cell lines. *Genomic instability* may lead to variation in the cell's genome as the number of passages increase, due to chromosomal aberrations acquired. Genomic alterations, for instance by loss of large fragments of chromosomes or mutations acquired, may result in change of the cell's characteristics compared to the parental tumor cells, leading to an altered proliferative potential in the human cancer cell line [85, 88]. Furthermore, culture conditions do not resemble that of the tumor environment, but represents simplified physiological conditions and these conditions may not be optimal. In our study, we have cultured all of our cell lines with the same growth media to be able to compare the different cell lines. *Cross-contamination* between different cell lines and *infections* such as mycoplasma may also occur [85]. However, to ensure that these are not issues of concern, we have STR profiled (=fingerprinted) our cell stock and performed frequent testing for mycoplasma.

Despite promising results in preclinical testing, the results in clinical studies are often disappointing and/or the toxicities are intolerable. Multiple theories have been proposed to explain the discrepancies between preclinical and clinical results. For instance, preclinical cytotoxicity assays are often not performed in an appropriate and optimal manner. Many *in vitro* studies are based on MTS assays measuring cellular viability after a few days with drug treatment. However, "viability" implies a measurement of both "live" and "dead" cells, while the MTS assay only reports the number of viable cells rather than measuring the relationship between "live" and "dead" cells or the decrease in metabolic activity. The number of cells plated, the concentration of the drug used and the time allowed for the drug to exert its effect are all factors that may affect the output of the assay [89]. In addition, other tumorigenic factors, such as differentiation and vascularization, are not considered.

Another issue is that *in vitro* studies often involve a limited number of cell lines. Furthermore, the number of cells treated *in vitro* is low compared to the number of cells in *in vivo* tumors (which are also more heterogeneous). Moreover, in *in vitro* cytotoxicity assays cells are often exposed to drug continuously, whereas patients receive a bolus dose and the concentration of drug that hits the tumor remains unknown. Additionally, in *in vitro* studies, cell lines are

monitored for a limited duration following drug treatment, whereas patients are followed up for months, revealing a possible acquired resistance to treatment. This suggests extension of cytotoxicity assay to a second stage of preclinical testing before introducing novel drugs to *in vivo* animal models and subsequently in human [89].

Time-lapse microscopy allows the monitoring of cell growth by examining cell density, which is affected by the number of cells, but also depends on cell morphology. However, since some cells undergo extensive morphological changes following treatment, this can mistakenly be displayed as an increased cell density. Morphological changes do not necessarily correlate with cell growth inhibition, and a cell can still be viable and its growth capacity not affected by the drug even though the morphology is changed. In our study, the visual inspection of phase-contrast images of the cells were performed to confirm the results obtained in the preceding cell growth assays.

5.2 Vemurafenib sensitivity in sarcoma cell lines

The inhibitory potential of the B-RAF^{V600E} inhibitor, vemurafenib, was investigated in four sarcoma cell lines with the B-RAF mutation: Two liposarcoma (SA-4 and SW872), one synovial sarcoma (SW982) and one Ewing's sarcoma (A673). A dose-dependent growth inhibition was observed for SA-4 and SW982 cells following treatment with vemurafenib. This result is consistent with the dose-response reported in melanomas treated with vemurafenib, both in *in vitro* and in *in vivo* models [50, 90]. Previously, the B-RAF^{V600E} mutation was found in several patients with clear cell sarcoma [80]. In a case study, a clear cell sarcoma patient responded to vemurafenib treatment, and a complete tumor regression of lung metastases was observed after eight weeks of treatment [81]. However, clear cell sarcoma tumors share histological properties and also molecular characteristics with melanoma tumors, and the distinction between the classification of these tumor types remains vague [82, 91]. Therefore, the observed efficacy of vemurafenib in clear cell sarcomas may be due to its near genetic relation to melanomas. The B-RAF^{V600E} mutation has also been described in several patients with gastrointestinal stromal tumor (GIST) [92]. Interestingly, another newer inhibitor targeting B-RAF^{V600E} (dabrafenib) has been reported and showed antitumor activity in a GIST patient [79].

Initially, all the cell lines included in this study were treated with vemurafenib (40 nM – 10 µM). However, following treatment of LPS510 cells which lack the B-RAF^{V600E} mutation, a reduction

in cell growth was observed only for the highest concentration of drug. This is likely a consequence of vemurafenib targeting B-RAF^{WT} since the inhibitor has affinity to both B-RAF^{V600E} and B-RAF^{WT}, although 10 times less efficient for the B-RAF^{WT} [55, 56, 93]. We therefore treated our cell lines with concentrations up to 5 µM, although higher concentrations of vemurafenib have been used for melanoma cell lines [94, 95].

Since SA-4 was the cell line with the greatest response to vemurafenib, we further investigated the cause of the growth inhibitory effect on these cells. Treatment of SA-4 cells with vemurafenib induced caspases-3/-7 activity and cell death only in a subset of cells at higher concentrations (**Figure 4.5**). A high level of cell death was, however, observed following treatment with vemurafenib for a longer duration (**Figure 4.6 & 4.7**), most likely indicating other mechanism for cell death such as necrosis. There is also a possibility that cells can induce apoptosis, for instance following a long-term cell arrest. Furthermore, cell cycle distribution of SA-4 cells following treatment with vemurafenib revealed cell cycle arrest in G_0/G_1-phase. This was also previously reported for melanoma cell lines following treatment with vemurafenib [50, 93, 96]. Interestingly, cells with a reduced amount of DNA than expected for diploid cells were observed in a dose-dependent manner following vemurafenib treatment. These cells were presented as a broadening of the left "shoulder" of the G_1-peak (called "sub-G_1") in the histogram, representing the cell cycle distribution (**Figure 4.6A**). Cells in sub-G_1 may also be necrotic cells (which have looser DNA conformation and thereby bind Hoechst less effectively) or early apoptotic cells. Apoptotic cells have lost a large fraction of their DNA and will appear as a separate peak. Moreover, it has been reported that cells in sub-G_1 may be a result of mechanical stress. Some cells may be more sensitive to mechanical stress following drug treatment. When cells are vortexed which is a part of the protocol, DNA conformation may be affected which can lead to reduced Hoechst binding and subsequently cells in sub-G_1 [97, 98].

Next, we assessed whether the inhibitory effect of vemurafenib on SA-4 cells was reversible. Following long term vemurafenib treatment (up to 310 hours), the majority of the cells were dead. However, upon removal of vemurafenib (and the dead cells), the remaining viable cells started to grow again. This was the case also after cells were exposed to the highest concentration of drug (5 µM) for 310 hours. This result is consistent with a previous study

reporting that cells were able to enter a slowly cycling drug-resistant state [99], indicating the need for continuous vemurafenib treatment.

5.3 Resistance to B-RAF inhibition

It is a well-known phenomenon that some melanoma patients are resistant to vemurafenib treatment, either initially (known as intrinsic resistance) or developed over time (acquired resistance) [99-101]. Acquired resistance to treatment in melanoma patients with the B-RAF^{V600E} mutation will normally occur approximately six months after initiated treatment with B-RAF^{V600E} targeted therapy [59, 93, 99, 102]. Likewise, a resistance to vemurafenib treatment is also observed for CRC patients [103]. In the present study, a resistance was observed for A673 and SW872 following treatment with both vemurafenib and RO5126766.

5.3.1 Mechanisms of resistance

Several resistance mechanisms have been proposed, including reactivation of the MAPK pathway, up-regulation of epidermal growth factor receptors (EGFRs) and/or other receptor tyrosine kinases (RTKs), splice variants of B-RAF^{V600E}, mutations in RAS GTPase and activation of the PI3K pathway [57, 101, 104].

Following treatment of the sarcoma cells in our study with either vemurafenib or RO5126766, a strong reduction of p-ERK was observed following treatment with either inhibitor (**Figure 4.8**). However, the cells were only treated for 3 hours. A recent *in vitro* study conducting a similar assay for a longer duration (24-48 hours), reported a re-accumulation of phosphorylated ERK following vemurafenib treatment in colorectal cancer (CRC) [73, 105]. Investigation revealed that inhibition of the B-RAF^{V600E} mutation in CRC cell lines can lead to an overexpression of EGFR/erbB–receptors. When B-RAF is inhibited, EGFR may activate RAS (RAS-GTP) to further phosphorylate C-RAF eventually re-phosphorylating ERK, and thereby bypass the loss of constitutively active B-RAF upon inhibition [73]. For colorectal cancer patients, vemurafenib treatment as monotherapy was not successful, whereas vemurafenib in combination with EGFR-inhibitors led to sustained p-ERK suppression [69, 73]. Interestingly, sequencing data for SW872 revealed the highest mRNA expression of EGFR (erbB1/HER1) in this cell line compared to the other eleven sequenced sarcoma cell lines (**Table 5.1** and data not shown). This may explain the low response observed in these cells following vemurafenib treatment [73]. However, a recent

study conducting similar assays reported a significant response to vemurafenib in SW872 cells [22]. This inconsistency may be a consequence of differences in culturing conditions and/or number of cells used in the experiments, which can affect the output.

SA-4 cells were also analyzed with regard to EGFR mRNA expression. Interestingly, sequencing data of this cell line revealed no/low mRNA levels of EGFR but high levels of erbB3/HER3, one of four members of the EGFR family of RTKs [106]. ErbB3 has low intrinsic kinase activity and is dependent of dimerization with another erbB-receptor to become activated, most importantly erbB2/HER2 [107, 108]. Since SA-4 cells express low amounts of erbB2-receptors, the EGFR-mediated reactivation of MAPK pathway is unlikely to occur. However, a resistance may occur following long term vemurafenib treatment of SA-4 cells, for instance by up-regulation of erbB2-receptors. This can potentially lead to hetero-dimerization of erbB2/erbB3-receptors and subsequently reactivation of the MAPK pathway.

The reactivation of MAPK signaling pathway is considered to be a central resistance mechanism [109-111]. In cells that harbor the B-RAF^{V600E} mutation, selective inhibitors block the signaling in this pathway. However, in cells with B-RAF^{WT}, a paradoxical reactivation of the signaling pathway occurs through a RAS-dependent dimerization of non-mutated RAF isoforms [55, 64, 65]. This occurs most commonly through hetero-dimerization (B-RAF/C-RAF) or homo-dimerization (C-RAF/C-RAF). Heterodimers which are most efficient at phosphorylating downstream kinases, compared to B-RAF^{V600E} mutated kinases which signal as a monomer [55, 112-114]. RAS-GTP activates C-RAF which upon dimerization is phosphorylated at its S338 residue further leading to downstream activation of the MAPK pathway [65, 115]. Long term treatment of melanoma patients with vemurafenib is believed to develop such secondary resistance resulting in tumor progression [110, 116]. The cell lines tested in the present study were treated for shorter durations. Interestingly, a paradoxical stimulation of cell growth was observed for LPS510 cells following treatment with low concentrations of either vemurafenib or RO5126766. Since this cell line lacks the B-RAF^{V600E} mutation, the effect of treatment may be a consequence of activation of MAPK pathway (**Figure 4.2 & 4.9**).

Splice variants of B-RAF^{V600E} are proteins with lower molecular weight due to for instance loss of a domain, subsequently rendering the B-RAF protein shorter than the full length protein. Such splice variants have been discovered in vemurafenib-resistant cells and is suggested as a

mechanism of resistance to RAF inhibitors [47, 117]. Some vemurafenib-resistant cells express a B-RAF^{V600E} variant with a molecular weight of approximately 61 kDa unlike the full length B-RAF protein which has a molecular weight of 84 kDa. Furthermore, a subset of cells with spliced variants of B-RAF^{V600E} lacks the RAS–binding domain. However, cells that express these shortened proteins have higher catalytic activity and induce dimerization in a RAS-independent manner in contrast to their full-length counterparts which require stimulation by RAS [47]. We did not observe a band at 61 kDa in our immunoblot when investigating the presence of B-RAF^{V600E} mutation in our cell lines (data not shown). However, we observed a band at approximately 75 kDa which is consistent with a previous study reporting this finding. This would suggest another splice variant of B-RAF with the mutated domain [118]. However, since the band was observed also in LPS510 which lacks the B-RAF^{V600E} mutation, it is more likely that the band occurs due to unspecific binding of another protein in the cell lysate.

Although the development of secondary mutations in cancer frequently causes resistance to targeted therapy, there is no evidence of such mutations in *B-RAF* following treatment with inhibitors targeting the B-RAF^{V600E} mutated protein [104, 109, 119]. Instead, activating mutations in RAS (most commonly in *KRAS* and *NRAS*) frequently occur in some cancer subtypes [119]. RAS activates the MAPK pathway, but is also an activating component of another signaling pathway involved in essential cellular processes, the phosphoinositide 3-kinase (PI3K) pathway. Therefore, cells that harbor RAS mutations, may lead to a constitutively active PI3K pathway [120-122]. The SA-4 and SW872 cell lines tested in our study do not harbor any K-RAS or N-RAS mutations (data not shown), which is consistent with the fact that mutations in *B-RAF* and *RAS* are normally not present in the same cell. However, the mutations may be present within different cells within the same tumor, which can lead to resistance to treatment [16, 57]. Such resistance may arise due to inhibition of the B-RAF^{V600E} mutation, which can further lead to up-regulation of N-RAS. The switching among the three RAF isoforms further allows N-RAS to signal to MEK-ERK through A-RAF and C-RAF, eventually leading to reactivation of the MAPK pathway [116, 119]. Interestingly, mRNA sequencing data of SW872 revealed higher expression of A-RAF and C-RAF compared to SA-4 (**Table 5.1**). Furthermore, a resistance may develop as a consequence of MAPK pathway inhibition, further leading to a RAS-mediated up-regulation of the PI3K pathway [123]. The interaction between several

pathways as well as the up-regulation of one pathway by another, suggests co-targeting of several pathways to overcome resistance.

Table 5.1. Endogenous mRNA expression			
Gene name	**SA-4**	**SW872**	**LPS510**
A-RAF	9.02	24.13	21.67
B-RAF	8.22	8.98	2.68
C-RAF/Raf-1	18.98	26.50	33.3
EGFR (erbB1)	0.02	56.58	15.9
ErbB2	12.89	11.25	12.6
ErbB3	98.40	0.03	0.14
ErbB4	0.01	0.01	0
K-RAS	8.76	11.76	8.15
N-RAS	30.04	38.26	46.18

Gene expression is evaluated as RPKM values (Reads Per Kilobase Million) and based on mRNA sequencing data.

5.4 Co-targeting multiple components

It was beyond the scope of this study to investigate combination therapies targeting several pathways. However, several studies have reported the benefit of integrating simultaneous B-RAF and MEK inhibition in melanomas to overcome resistance [119]. Since A673 and SW872 cells were relatively resistant to vemurafenib treatment, all the four sarcoma cell lines were also treated with the inhibitor RO5126766, which targets both RAF and MEK1-kinases. Our hypothesis was that if inhibition of B-RAF^{V600E} was not sufficient, co-inhibition of a kinase downstream of B-RAF in addition might demonstrate a more significant inhibition of growth. This way, cells would not be able to bypass MAPK activation. However, treatment with the dual inhibitor did not exert any stronger growth inhibition compared to that observed for vemurafenib, for any of the tested cell lines. Taking into account the results obtained in this thesis, further investigation are warranted to conclude about therapeutic potential of targeting the B-RAF^{V600E} mutation in sarcomas.

6 Conclusion

In this study, the efficacy of the MAPK pathway inhibitors, vemurafenib and RO5126766 (targeting B-RAF^{V600E} and RAF/MEK1 respectively) was evaluated in selected sarcoma cell lines. Both vemurafenib and RO5126766 inhibited cell growth in SA-4 and SW982 cells, although the effect was not significant for the latter cell line. The A673 and SW872 cells were resistant to treatment with either of the tested inhibitors. In SA-4 cells, vemurafenib induced a small degree of apoptosis and a more pronounced G_0/G_1 cell cycle arrest following vemurafenib treatment. However, the resumed growth of cells following removal of vemurafenib indicated a reversible inhibitory effect. Treatment with RO5126766, targeting two kinases in the same MAPK pathway, did not exert a greater response than vemurafenib in the short-term assays performed in the present study. This indicates that the sarcoma cell lines tested in this study may not be dependent of B-RAF and MEK for their proliferation and it is likely that other pathways, e.g. EGF signaling and PI3K pathway, are more essential for these cells. Taking into account the low frequency of B-RAF – mutated sarcomas combined with low efficacy of B-RAF inhibitors in the B-RAF mutated tested cell lines, targeting of the B-RAF mutation may not be the future path to investigate.

7 Future perspectives

1. Although B-RAF, and MAPK pathway in general, do not seem to be essential for the cell lines investigated in our study, it would be interesting to test different intra-pathway combinations as well as inhibitors that affect ERK kinase directly.

2. As revealed in mRNA sequencing data for SW872, EGFR is highly expressed. Inhibition of EGF signaling may therefore be of relevance in such case.

3. In some cancers, the inhibition of a particular pathway may activate other pathways in the cell, for instance the PI3K/mTOR/AKT-pathway. Efficacy of PI3K inhibition in combination with MAPK inhibitors should be investigated, especially in cells that harbor RAS mutations.

4. The potential of sequential inhibition should be assessed in sarcoma cell lines, e.g. treating cells with vemurafenib and thereafter with, for instance, a MEK inhibitor.

5. The therapeutic potential of the pan-inhibitor (affinity to all the RAF isoforms), TAK-632, which has showed effectiveness in colorectal cancers resistant to vemurafenib treatment, should also be assessed in the resistant sarcoma cell lines in the present study.

6. Since there is a possibility that cells may acquire new mutations over time following treatment (e.g. RAS mutations), the cells should be sequenced with regard to genetic alterations post-treatment.

References

1. Ferlay, J., et al., *Cancer incidence and mortality worldwide: Sources, methods and major patterns in GLOBOCAN 2012.* International Journal of Cancer, 2015. **136**(5): p. E359-E386.
2. Gatta, G., et al., *Rare cancers are not so rare: The rare cancer burden in Europe.* European Journal of Cancer, 2011. **47**(17): p. 2493-2511.
3. Burningham, Z., et al., *The Epidemiology of Sarcoma.* Clinical Sarcoma Research, 2012. **2**: p. 14-14.
4. Stratton, M.R., *Exploring the Genomes of Cancer Cells: Progress and Promise.* Science, 2011. **331**(6024): p. 1553-1558.
5. Yates, L.R. and P.J. Campbell, *Evolution of the cancer genome.* Nat Rev Genet, 2012. **13**(11): p. 795-806.
6. Ponder, B.A., *Molecular genetics of cancer.* BMJ, 1992. **304**(6836): p. 1234-6.
7. Vogelstein, B. and K.W. Kinzler, *Cancer genes and the pathways they control.* Nat Med, 2004. **10**(8): p. 789-799.
8. Lengauer, C., K.W. Kinzler, and B. Vogelstein, *Genetic instabilities in human cancers.* Nature, 1998. **396**(6712): p. 643-649.
9. Stratton, M.R., P.J. Campbell, and P.A. Futreal, *The cancer genome.* Nature, 2009. **458**(7239): p. 719-724.
10. Nambiar, M., V. Kari, and S.C. Raghavan, *Chromosomal translocations in cancer.* Biochimica et Biophysica Acta (BBA) - Reviews on Cancer, 2008. **1786**(2): p. 139-152.
11. Garnett, M.J. and R. Marais, *Guilty as charged: B-RAF is a human oncogene.* Cancer Cell, 2004. **6**(4): p. 313-319.
12. Komarova, N.L., A. Sengupta, and M.A. Nowak, *Mutation–selection networks of cancer initiation: tumor suppressor genes and chromosomal instability.* Journal of Theoretical Biology, 2003. **223**(4): p. 433-450.
13. Rivlin, N., et al., *Mutations in the p53 Tumor Suppressor Gene: Important Milestones at the Various Steps of Tumorigenesis.* Genes & Cancer, 2011. **2**(4): p. 466-474.
14. Hanahan, D. and Robert A. Weinberg, *Hallmarks of Cancer: The Next Generation.* Cell, 2011. **144**(5): p. 646-674.
15. Davies, M.A. and Y. Samuels, *Analysis of the genome to personalize therapy for melanoma.* Oncogene, 2010. **29**(41): p. 5545-5555.
16. Davies, H., et al., *Mutations of the BRAF gene in human cancer.* Nature, 2002. **417**(6892): p. 949-954.
17. Cohen, G.M., *Caspases: the executioners of apoptosis.* Biochemical Journal, 1997. **326**(Pt 1): p. 1-16.
18. Zahm, S.H. and J. Fraumeni. *The epidemiology of soft tissue sarcoma*. in *Seminars in oncology*. 1997. WB SAUNDERS CO INDEPENDENCE SQUARE WEST CURTIS CENTER, STE 300, PHILADELPHIA, PA 19106-3399.
19. Fletcher, C., K. Unni, and F. Mertens, *World health organization classification of tumours. Pathology and genetics of tumours of soft tissue and bone. IARC Press.* Lyon, 2002: p. 2002.

20. Anderson, J.L., et al., *Pediatric Sarcomas: Translating Molecular Pathogenesis of Disease to Novel Therapeutic Possibilities.* Pediatric research, 2012. **72**(2): p. 112-121.
21. Clark , M.A., et al., *Soft-Tissue Sarcomas in Adults.* New England Journal of Medicine, 2005. **353**(7): p. 701-711.
22. Kanojia, D., et al., *Genomic landscape of liposarcoma.* Oncotarget, 2015. **6**(40): p. 42429-42444.
23. Forus, A., et al., *Dedifferentiation of a well-differentiated liposarcoma to a highly malignant metastatic osteosarcoma:: amplification of 12q14 at all stages and gain of 1q22–q24 associated with metastases.* Cancer Genetics and Cytogenetics, 2001. **125**(2): p. 100-111.
24. Siegel, R.L., K.D. Miller, and A. Jemal, *Cancer statistics, 2017.* CA: A Cancer Journal for Clinicians, 2017. **67**(1): p. 7-30.
25. Williams, R.F., I. Fernandez-Pineda, and A. Gosain, *Pediatric Sarcomas.* Surgical Clinics of North America, 2016. **96**(5): p. 1107-1125.
26. Cormier, J.N. and R.E. Pollock, *Soft Tissue Sarcomas.* CA: A Cancer Journal for Clinicians, 2004. **54**(2): p. 94-109.
27. Xue, Y. and W.R. Wilcox, *Changing paradigm of cancer therapy: precision medicine by next-generation sequencing.* Cancer Biology & Medicine, 2016. **13**(1): p. 12-18.
28. Kou, T., et al., *The possibility of clinical sequencing in the management of cancer.* Japanese Journal of Clinical Oncology, 2016. **46**(5): p. 399-406.
29. Tamborero, D., et al., *Comprehensive identification of mutational cancer driver genes across 12 tumor types.* Scientific Reports, 2013. **3**: p. 2650.
30. Henkes, M., H. van der Kuip, and W.E. Aulitzky, *Therapeutic options for chronic myeloid leukemia: focus on imatinib (Glivec(®), Gleevec™).* Therapeutics and Clinical Risk Management, 2008. **4**(1): p. 163-187.
31. Iqbal, N. and N. Iqbal, *Imatinib: A Breakthrough of Targeted Therapy in Cancer.* Chemotherapy Research and Practice, 2014. **2014**: p. 9.
32. Dagher, R., et al., *Approval Summary.* Imatinib Mesylate in the Treatment of Metastatic and/or Unresectable Malignant Gastrointestinal Stromal Tumors, 2002. **8**(10): p. 3034-3038.
33. Wellbrock, C., M. Karasarides, and R. Marais, *The RAF proteins take centre stage.* Nat Rev Mol Cell Biol, 2004. **5**(11): p. 875-885.
34. McCubrey, J.A., et al., *Roles of the Raf/MEK/ERK pathway in cell growth, malignant transformation and drug resistance.* Biochim Biophys Acta, 2007. **1773**(8): p. 1263-84.
35. Ascierto, P.A., et al., *The role of BRAF V600 mutation in melanoma.* Journal of Translational Medicine, 2012. **10**: p. 85-85.
36. Katz, M., I. Amit, and Y. Yarden, *Regulation of MAPKs by growth factors and receptor tyrosine kinases.* Biochimica et biophysica acta, 2007. **1773**(8): p. 1161-1176.
37. Santarpia, L., S.L. Lippman, and A.K. El-Naggar, *Targeting the Mitogen-Activated Protein Kinase RAS-RAF Signaling Pathway in Cancer Therapy*. Expert opinion on therapeutic targets, 2012. **16**(1): p. 103-119.
38. Nolen, B., S. Taylor, and G. Ghosh, *Regulation of Protein Kinases: Controlling Activity through Activation Segment Conformation.* Molecular Cell, 2004. **15**(5): p. 661-675.
39. Tran, N.H., X. Wu, and J.A. Frost, *B-Raf and Raf-1 Are Regulated by Distinct Autoregulatory Mechanisms.* Journal of Biological Chemistry, 2005. **280**(16): p. 16244-16253.

40. Emuss, V., et al., *Mutations of C-RAF Are Rare in Human Cancer because C-RAF Has a Low Basal Kinase Activity Compared with B-RAF*. Cancer Research, 2005. **65**(21): p. 9719-9726.
41. Wilson, M.A., et al., *What you are missing could matter: a rare, complex BRAF mutation affecting codons 599, 600, and 601 uncovered by next generation sequencing.* Cancer Genetics, 2014. **207**(6): p. 272-275.
42. Halilovic, E. and D.B. Solit, *Therapeutic strategies for inhibiting oncogenic BRAF signaling.* Current Opinion in Pharmacology, 2008. **8**(4): p. 419-426.
43. McCain, J., *The MAPK (ERK) Pathway: Investigational Combinations for the Treatment Of BRAF-Mutated Metastatic Melanoma.* Pharmacy and Therapeutics, 2013. **38**(2): p. 96-108.
44. Wan, P.T.C., et al., *Mechanism of Activation of the RAF-ERK Signaling Pathway by Oncogenic Mutations of B-RAF*. Cell, 2004. **116**(6): p. 855-867.
45. Bollag, G., et al., *Vemurafenib: the first drug approved for BRAF-mutant cancer.* Nat Rev Drug Discov, 2012. **11**(11): p. 873-886.
46. Satyamoorthy, K., et al., *Constitutive Mitogen-activated Protein Kinase Activation in Melanoma Is Mediated by Both BRAF Mutations and Autocrine Growth Factor Stimulation.* Cancer Research, 2003. **63**(4): p. 756-759.
47. Poulikakos, P.I., et al., *RAF inhibitor resistance is mediated by dimerization of aberrantly spliced BRAF(V600E).* Nature, 2011. **480**(7377): p. 387-390.
48. Niault, T.S. and M. Baccarini, *Targets of Raf in tumorigenesis.* Carcinogenesis, 2010. **31**(7): p. 1165-1174.
49. Eisen, T., et al., *Sorafenib in advanced melanoma: a Phase II randomised discontinuation trial analysis.* British Journal of Cancer, 2006. **95**(5): p. 581-586.
50. Yang, H., et al., *RG7204 (PLX4032), a Selective BRAFV600E Inhibitor, Displays Potent Antitumor Activity in Preclinical Melanoma Models.* Cancer Research, 2010. **70**(13): p. 5518-5527.
51. Bollag, G., et al., *Clinical efficacy of a RAF inhibitor needs broad target blockade in BRAF-mutant melanoma.* Nature, 2010. **467**(7315): p. 596-599.
52. Keating, G.M. and K.A. Lyseng-Williamson, *Vemurafenib.* American Journal of Clinical Dermatology, 2013. **14**(1): p. 65-69.
53. Joseph, E.W., et al., *The RAF inhibitor PLX4032 inhibits ERK signaling and tumor cell proliferation in a V600E BRAF-selective manner.* Proceedings of the National Academy of Sciences of the United States of America, 2010. **107**(33): p. 14903-14908.
54. Holderfield, M., et al., *Targeting RAF kinases for cancer therapy: BRAF mutated melanoma and beyond.* Nature reviews. Cancer, 2014. **14**(7): p. 455-467.
55. Poulikakos, P.I., et al., *RAF inhibitors transactivate RAF dimers and ERK signalling in cells with wild-type BRAF*. Nature, 2010. **464**(7287): p. 427-430.
56. Tsai, J., et al., *Discovery of a selective inhibitor of oncogenic B-Raf kinase with potent antimelanoma activity.* Proceedings of the National Academy of Sciences, 2008. **105**(8): p. 3041-3046.
57. Fisher, R. and J. Larkin, *Vemurafenib: a new treatment for BRAF-V600 mutated advanced melanoma.* Cancer Management and Research, 2012. **4**: p. 243-252.
58. Sosman , J.A., et al., *Survival in BRAF V600–Mutant Advanced Melanoma Treated with Vemurafenib.* New England Journal of Medicine, 2012. **366**(8): p. 707-714.

59. Flaherty , K.T., et al., *Inhibition of Mutated, Activated BRAF in Metastatic Melanoma.* New England Journal of Medicine, 2010. **363**(9): p. 809-819.
60. Chapman , P.B., et al., *Improved Survival with Vemurafenib in Melanoma with BRAF V600E Mutation.* New England Journal of Medicine, 2011. **364**(26): p. 2507-2516.
61. Sun, W. and L.M. Schuchter, *Metastatic melanoma.* Current Treatment Options in Oncology, 2001. **2**(3): p. 193-202.
62. Larkin, J., et al., *Vemurafenib in patients with BRAFV600 mutated metastatic melanoma: an open-label, multicentre, safety study.* The Lancet Oncology, 2014. **15**(4): p. 436-444.
63. McArthur, G.A., et al., *Safety and efficacy of vemurafenib in BRAF(V600E) and BRAF(V600K) mutation-positive melanoma (BRIM-3): extended follow-up of a phase 3, randomised, open-label study.* The Lancet. Oncology, 2014. **15**(3): p. 323-332.
64. Hatzivassiliou, G., et al., *RAF inhibitors prime wild-type RAF to activate the MAPK pathway and enhance growth.* Nature, 2010. **464**(7287): p. 431-435.
65. Heidorn, S.J., et al., *Kinase-Dead BRAF and Oncogenic RAS Cooperate to Drive Tumor Progression through CRAF.* Cell. **140**(2): p. 209-221.
66. Lacouture, M.E., et al., *Induction of Cutaneous Squamous Cell Carcinomas by RAF Inhibitors: Cause for Concern?* Journal of Clinical Oncology, 2012. **30**(3): p. 329-330.
67. Oberholzer, P.A., et al., *RAS Mutations Are Associated With the Development of Cutaneous Squamous Cell Tumors in Patients Treated With RAF Inhibitors.* Journal of Clinical Oncology, 2012. **30**(3): p. 316-321.
68. da Rocha Dias, S., et al., *The European Medicines Agency review of vemurafenib (Zelboraf®) for the treatment of adult patients with BRAF V600 mutation-positive unresectable or metastatic melanoma: Summary of the scientific assessment of the Committee for Medicinal Products for Human Use.* European Journal of Cancer, 2013. **49**(7): p. 1654-1661.
69. Yang, H., et al., *Antitumor Activity of BRAF Inhibitor Vemurafenib in Preclinical Models of BRAF-Mutant Colorectal Cancer.* Cancer Research, 2012. **72**(3): p. 779-789.
70. Clarke, C.N. and E.S. Kopetz, *BRAF mutant colorectal cancer as a distinct subset of colorectal cancer: clinical characteristics, clinical behavior, and response to targeted therapies.* Journal of Gastrointestinal Oncology, 2015. **6**(6): p. 660-667.
71. Barras, D., *BRAF Mutation in Colorectal Cancer: An Update.* Biomarkers in Cancer, 2015. **7**(Suppl 1): p. 9-12.
72. Czarniecka, A., M. Oczko-Wojciechowska, and M. Barczyński, *BRAF V600E mutation in prognostication of papillary thyroid cancer (PTC) recurrence.* Gland Surgery, 2016. **5**(5): p. 495-505.
73. Corcoran, R.B., et al., *EGFR-Mediated Reactivation of MAPK Signaling Contributes to Insensitivity of BRAF-Mutant Colorectal Cancers to RAF Inhibition with Vemurafenib.* Cancer Discovery, 2012. **2**(3): p. 227-235.
74. Moorcraft, S.Y., E.C. Smyth, and D. Cunningham, *The role of personalized medicine in metastatic colorectal cancer: an evolving landscape.* Therapeutic Advances in Gastroenterology, 2013. **6**(5): p. 381-395.
75. Kopetz, S., et al., *Phase II Pilot Study of Vemurafenib in Patients With Metastatic BRAF-Mutated Colorectal Cancer.* Journal of Clinical Oncology, 2015. **33**(34): p. 4032-4038.
76. Kopetz, S., et al., *PLX4032 in metastatic colorectal cancer patients with mutant BRAF tumors.* Journal of Clinical Oncology, 2010. **28**(15_suppl): p. 3534-3534.

77. De Roock, W., et al., *Effects of KRAS, BRAF, NRAS, and PIK3CA mutations on the efficacy of cetuximab plus chemotherapy in chemotherapy-refractory metastatic colorectal cancer: a retrospective consortium analysis.* The Lancet Oncology. **11**(8): p. 753-762.
78. Jonker , D.J., et al., *Cetuximab for the Treatment of Colorectal Cancer.* New England Journal of Medicine, 2007. **357**(20): p. 2040-2048.
79. Falchook, G.S., et al., *BRAF Mutant Gastrointestinal Stromal Tumor: First report of regression with BRAF inhibitor dabrafenib (GSK2118436) and whole exomic sequencing for analysis of acquired resistance.* Oncotarget, 2013. **4**(2): p. 310-315.
80. Park, B.M., et al., *Two cases of clear cell sarcoma with different clinical and genetic features: cutaneous type with BRAF mutation and subcutaneous type with KIT mutation.* British Journal of Dermatology, 2013. **169**(6): p. 1346-1352.
81. Protsenko, S.A., et al., *BRAF-mutated clear cell sarcoma is sensitive to vemurafenib treatment.* Investigational New Drugs, 2015. **33**(5): p. 1136-1143.
82. Hocar, O., et al., *Clear Cell Sarcoma (Malignant Melanoma) of Soft Parts: A Clinicopathologic Study of 52 Cases.* Dermatology Research and Practice, 2012. **2012**: p. 8.
83. Ishii, N., et al., *Enhanced Inhibition of ERK Signaling by a Novel Allosteric MEK Inhibitor, CH5126766, That Suppresses Feedback Reactivation of RAF Activity.* Cancer Research, 2013. **73**(13): p. 4050-4060.
84. Wada, M., et al., *The Dual RAF/MEK Inhibitor CH5126766/RO5126766 May Be a Potential Therapy for RAS-Mutated Tumor Cells.* PLOS ONE, 2014. **9**(11): p. e113217.
85. van Staveren, W.C.G., et al., *Human cancer cell lines: Experimental models for cancer cells in situ? For cancer stem cells?* Biochimica et Biophysica Acta (BBA) - Reviews on Cancer, 2009. **1795**(2): p. 92-103.
86. Jung, J., *Human Tumor Xenograft Models for Preclinical Assessment of Anticancer Drug Development.* Toxicological Research, 2014. **30**(1): p. 1-5.
87. Gao, H., et al., *High-throughput screening using patient-derived tumor xenografts to predict clinical trial drug response.* Nat Med, 2015. **21**(11): p. 1318-1325.
88. Becerikli, M., et al., *Growth rate of late passage sarcoma cells is independent of epigenetic events but dependent on the amount of chromosomal aberrations.* Experimental Cell Research, 2013. **319**(12): p. 1724-1731.
89. Eastman, A., *Improving anticancer drug development begins with cell culture: misinformation perpetrated by the misuse of cytotoxicity assays.* Oncotarget, 2017. **8**(5): p. 8854-8866.
90. Sala, E., et al., *BRAF Silencing by Short Hairpin RNA or Chemical Blockade by PLX4032 Leads to Different Responses in Melanoma and Thyroid Carcinoma Cells.* Molecular Cancer Research, 2008. **6**(5): p. 751-759.
91. Uguen, A., P. Marcorelles, and M. De Braekeleer, *Targeting BRAF mutants in clear-cell sarcomas of soft tissue: beyond sarcoma or melanoma classification.* Investigational New Drugs, 2016. **34**(2): p. 253-254.
92. Hostein, I., et al., *BRAF Mutation Status in Gastrointestinal Stromal Tumors.* American Journal of Clinical Pathology, 2010. **133**(1): p. 141-148.
93. Kim, A. and M.S. Cohen, *The discovery of vemurafenib for the treatment of BRAF-mutated metastatic melanoma.* Expert Opinion on Drug Discovery, 2016. **11**(9): p. 907-916.

94. Koya, R.C., et al., *BRAF inhibitor vemurafenib improves the antitumor activity of adoptive cell immunotherapy.* Cancer research, 2012. **72**(16): p. 3928-3937.
95. Roos, W.P., et al., *B-Raf inhibitor vemurafenib in combination with temozolomide and fotemustine in the killing response of malignant melanoma cells.* Oncotarget, 2014. **5**(24): p. 12607-12620.
96. Lee, J.T., et al., *PLX4032, a Potent Inhibitor of the B-Raf V600E Oncogene, Selectively Inhibits V600E-positive Melanomas.* Pigment cell & melanoma research, 2010. **23**(6): p. 820-827.
97. Wlodkowic, D., et al., *Apoptosis and Beyond: Cytometry in Studies of Programmed Cell Death.* Methods in Cell Biology, 2011. **103**: p. 55-98.
98. Darzynkiewicz, Z., H.D. Halicka, and H. Zhao, *Analysis of Cellular DNA Content by Flow and Laser Scanning Cytometry.* Advances in experimental medicine and biology, 2010. **676**: p. 137-147.
99. Fallahi-Sichani, M., et al., *Adaptive resistance of melanoma cells to RAF inhibition via reversible induction of a slowly dividing de-differentiated state.* Molecular Systems Biology, 2017. **13**(1): p. 905.
100. Swaika, A., J.A. Crozier, and R.W. Joseph, *Vemurafenib: an evidence-based review of its clinical utility in the treatment of metastatic melanoma.* Drug Design, Development and Therapy, 2014. **8**: p. 775-787.
101. Manzano, J.L., et al., *Resistant mechanisms to BRAF inhibitors in melanoma.* Annals of Translational Medicine, 2016. **4**(12): p. 237.
102. Sun, C., et al., *Reversible and adaptive resistance to BRAF(V600E) inhibition in melanoma.* Nature, 2014. **508**(7494): p. 118-122.
103. Mao, M., et al., *Resistance to BRAF Inhibition in BRAF-Mutant Colon Cancer Can Be Overcome with PI3K Inhibition or Demethylating Agents.* Clinical Cancer Research, 2013. **19**(3): p. 657-667.
104. Villanueva, J., A. Vultur, and M. Herlyn, *Resistance to BRAF inhibitors: Unraveling mechanisms and future treatment options.* Cancer research, 2011. **71**(23): p. 7137-7140.
105. Prahallad, A., et al., *Unresponsiveness of colon cancer to BRAF(V600E) inhibition through feedback activation of EGFR.* Nature, 2012. **483**(7388): p. 100-103.
106. Ma, J., et al., *Targeting of erbB3 receptor to overcome resistance in cancer treatment.* Molecular Cancer, 2014. **13**(1): p. 105.
107. Schulze, W.X., L. Deng, and M. Mann, *Phosphotyrosine interactome of the ErbB-receptor kinase family.* Molecular Systems Biology, 2005. **1**: p. 2005.0008-2005.0008.
108. Shi, F., et al., *ErbB3/HER3 intracellular domain is competent to bind ATP and catalyze autophosphorylation.* Proc Natl Acad Sci U S A, 2010. **107**.
109. Yadav, V., et al., *Reactivation of Mitogen-activated Protein Kinase (MAPK) Pathway by FGF Receptor 3 (FGFR3)/Ras Mediates Resistance to Vemurafenib in Human B-RAF V600E Mutant Melanoma.* The Journal of Biological Chemistry, 2012. **287**(33): p. 28087-28098.
110. Gibney, G.T., et al., *Paradoxical oncogenesis and the long term consequences of BRAF inhibition in melanoma.* Nature reviews. Clinical oncology, 2013. **10**(7): p. 390-399.
111. Spagnolo, F., et al., *BRAF-mutant melanoma: treatment approaches, resistance mechanisms, and diagnostic strategies.* OncoTargets and therapy, 2015. **8**: p. 157-168.
112. Weber, C.K., et al., *Active Ras Induces Heterodimerization of cRaf and BRaf.* Cancer Research, 2001. **61**(9): p. 3595-3598.

113. Garnett, M.J., et al., *Wild-Type and Mutant B-RAF Activate C-RAF through Distinct Mechanisms Involving Heterodimerization.* Molecular Cell. **20**(6): p. 963-969.
114. Rushworth, L.K., et al., *Regulation and Role of Raf-1/B-Raf Heterodimerization.* Molecular and Cellular Biology, 2006. **26**(6): p. 2262-2272.
115. Zang, M., et al., *Characterization of Ser338 Phosphorylation for Raf-1 Activation.* Journal of Biological Chemistry, 2008. **283**(46): p. 31429-31437.
116. Villanueva, J., et al., *Acquired Resistance to BRAF Inhibitors Mediated by a RAF Kinase Switch in Melanoma Can Be Overcome by Cotargeting MEK and IGF-1R/PI3K.* Cancer Cell, 2010. **18**(6): p. 683-695.
117. Hartsough, E.J., K.J. Basile, and A.E. Aplin, *Beneficial Effects of RAF Inhibitor in Mutant BRAF Splice Variant–Expressing Melanoma.* Molecular Cancer Research, 2014. **12**(5): p. 795-802.
118. Capper, D., et al., *Assessment of BRAF V600E mutation status by immunohistochemistry with a mutation-specific monoclonal antibody.* Acta Neuropathologica, 2011. **122**(1): p. 11-19.
119. Nazarian, R., et al., *Melanomas acquire resistance to B-RAF(V600E) inhibition by RTK or N-RAS upregulation.* Nature, 2010. **468**(7326): p. 973-977.
120. Vara, J.Á.F., et al., *PI3K/Akt signalling pathway and cancer.* Cancer Treatment Reviews, 2004. **30**(2): p. 193-204.
121. Shi, H., et al., *Acquired resistance and clonal evolution in melanoma during BRAF inhibitor therapy.* Cancer discovery, 2014. **4**(1): p. 80-93.
122. Pacold, M.E., et al., *Crystal Structure and Functional Analysis of Ras Binding to Its Effector Phosphoinositide 3-Kinase γ.* Cell, 2000. **103**(6): p. 931-944.
123. Mendoza, M.C., E.E. Er, and J. Blenis, *The Ras-ERK and PI3K-mTOR Pathways: Cross-talk and Compensation.* Trends in biochemical sciences, 2011. **36**(6): p. 320-328.

Appendices

Appendix 1: Abbreviations

µ	Micro
µg	Microgram
µl	Microliter
µM	Micro molar
A-RAF	v-Raf murine sarcoma 3611 viral oncogene homolog 1
ATCC	American type culture collection
ATP	Adenosine triphosphate
B-RAF	v-Raf murine sarcoma viral oncogene homolog B
$B\text{-}RAF^{V600E}$	V600E-mutated B-RAF
$B\text{-}RAF^{WT}$	Wild-type B-RAF
CCS	Clear cell sarcoma
CML	Chronic myeloid leukemia
C-RAF/Raf-1	v-Raf-1 murine leukemia viral oncogene homolog 1
CRC	Colorectal cancer
DDLPS	Dedifferentiated liposarcoma
DMSO	Dimethyl sulfoxide
DNA	Deoxyribonucleic acid
EDTA	Ethylenediaminetetraacetic acid
EGF	Epidermal growth factor
EGFR	Epidermal growth factor receptor
ERK	Extracellular signal-regulated kinase
FBS	Fetal bovine serum
FDA	Food and drug administration
FSC	Forward scatter
g	Gravity
GDP	Guanosine diphosphate
GF	Growth factor
GIST	Gastrointestinal stromal tumor
GRB2	Growth factor receptor-bound 2
GTP	Guanosine triphosphate
GTPase	Guanosine triphosphatase
HER1	Human epidermal growth factor receptor 1
HRP	Horseradish peroxidase

kDa	Kilo Dalton
KIT	v-Kit Hardy Zuckerman 4 feline sarcoma viral oncogene
K-RAS	Kirsten rat sarcoma viral oncogene homolog
MAPK	Mitogen-activated protein kinase
mCRC	Metastatic colorectal cancer
MEK	Mitogen activated protein kinase kinase
mM	Milli molar
mRNA	Messenger RNA
n	Number of biological replicates
NGS	Next generation sequencing
nm	Nanometer
N-RAS	Neuroblastoma RAS viral oncogene homolog
PAGE	Polyacrylamide gel electrophoresis
PBS	Phosphate-buffered saline
PCR	Polymerase chain reaction
p-ERK	Phosphorylated ERK
PI3K	Phosphoinositide-3 kinase
PVDF	Polyvinylidene difluoride
RNA	Ribonucleic acid
RPKM	Reads per kilobase million
RT	Room temperature
RTK	Receptor tyrosine kinase
SCC	Squamous cell carcinoma
SD	Standard deviation
SDS	Sodium dodecyl sulphate
SEM	Standard error of mean
SOS	Sons of sevenless
SSC	Side scatter
STR	Short tandem repeat
STS	Soft tissue sarcoma
TBS	Tris-buffered saline
TP53	Tumor protein p53
UV	Ultraviolet
v/v	Volume/volume
α	Alpha
β	Beta

Appendix 2: Reagents

Product	Provider	Catalog number
RPMI-1640 medium	Sigma-Aldrich	R0883
Fetal bovine serum (FBS)	Sigma-Aldrich	F7524
Dulbeco's Phosphate-buffered saline (PBS)	Sigma-Aldrich	D8537
Glutamax ™ Supplement	Gibco ® by Life Technologies	35050-038
Trypsin-EDTA mixture (1X)	Sigma-Aldrich	T3924
Dimethyl sulfoxide (DMSO)	Sigma-Aldrich	D2650
Hybri-MAX™		
Trypan Blue Stain, 0.4 %	Life Technologies	T10282
PLX4032 (vemurafenib)	Selleckchem	S1267
RO5126766(CH5126766)	Selleckchem	57170
CellPlayer Kinetic Caspase-3/-7 reagent	Essen Bioscience	4440
Ethanol 96 %	VWR Chemicals	20824.296
MTS	Promega	G3582
Hoechst 33258	Sigma-Aldrich	94403
Penicillin Streptomycin 10 mg/ml	Sigma-Aldrich	P4458
Complete Mini (Protease inhibitors)	Roche	04693124001
PhoSTOP (Phosphatase inhibitors)	Roche	04906837001
Purified bovine serum albumin (BSA)	BioLabs	B9001S
10mg/ml		
Methanol 100 %	VWR Chemicals	20847.307
Bio-Rad protein assay dye	Bio-Rad	500-0006
NuPAGE ® 4-12 % Bis-Tris Gel, 1.0 mm x	Novex ® by Life technologies	NP0331
10 wells		
NuPAGE ® 4-12 % Bis-Tris Gel, 1.0 mm x	Novex ® by Life technologies	NP0332
12 wells		
NuPAGE ® 4-12 % Bis-Tris Gel, 1.0 mm x	Novex ® by Life technologies	NP0323BOX
15 wells		
NuPAGE ® MOPS SDS Running Buffer	Invitrogen	NP0001-02
(20 X)		
LDS sample buffer (4X)	Invitrogen	NP0008
Precision Plus Protein ® Dual Color	Bio-Rad	161-0374
Standards		
PVDF membrane (0.45µm pore size)	Whatman ®	3030-335
Chromatography paper		
Super Signal ® West Dura Extended	Thermo Scientific	34076
Duration Substrate		

Antibodies

Primary Antibodies **(Raised in)**	**Dilution/working concentration**	**Provider**	**Catalog number**
Anti-B-RAF^{V600E} (Rabbit)	1:1000	RevMAb Nordic Bioscience	31-1042-005
Anti-B-RAF (Rabbit)	1:200	Sigma-Aldrich	HPA001238
Anti-p-ERK (Rabbit)	1:1000	Cell-signaling	5370
Anti-ERK (Rabbit)	1:000	Cell-signaling	9102
Anti-α-tubulin (Mouse)	1:2000	CellBiochem	Cp06
Secondary antibodies			
Anti-mouse	1:5000 in 10 % non-fat dry milk	Dako	P0260
Anti-rabbit	1:5000 in 10 % Non-fat dry milk	Dako	P0448

Appendix 3: Solutions

Western blot	Ingredients/ Reagents	Stock concentration/ Volume/Amount	Final concentration/ volume
3x SDS lysis buffer	SDS	100%	3.2 %
	Trizma Base	100%	1 %
	Glycerol	100%	14 %
	B-mercaptoethanol	100%	7 %
	ddH_2O	Adjusted to desired volume	
1X SDS lysis buffer	Lysis buffer	333 µl of 3X	
	Protease inhibitor	143 µl of 7X	
	Phosphatase inhibitor	100 µl of 10X	
	PBS	424 µl	
Transfer buffer (10 X)	Tris	30.3 g	
	Glycin	144 g	
	ddH_2O	Adjusted to 1 L	
Transfer buffer (1X)	10 X Transfer buffer	100 ml	
	20 % methanol	200 ml	
	ddH_2O	Adjusted to 1 L	
Running buffer	MOPS running buffer	50 ml	
	ddH_2O	Adjust to 1 L	
Washing buffer (TBS-T)	NaCL	30 ml of 5M solution	150 mM
	Tris-HCL	20 ml of 1M solution	20 mM
	Tween-20	5 ml of 20 % solution	0.1 %
	ddH_2O	Adjusted to 1 L	
Development solution			
Super Signal ® West Dura Extended Duration Substrate	Stable peroxide solution	Equal parts	1:1
	Luminol/Enhancer solution		

Culturing			
Freezing media	FBS		90 %
	DMSO		10 %
Cell cycle analysis			
Staining buffer	PBS		Desired volume
	FBS		1 %
	Hoechst 33258		2 µg/ml